Am J Physiol Regul Integr Comp Physiol 300: R969–R977, 2011.
First published January 26, 2011; doi:10.1152/ajpregu.00768.2010.

Exercise training augments the dynamic heart rate response to vagal but not sympathetic stimulation in rats

Masaki Mizuno,[1,2] Toru Kawada,[2] Atsunori Kamiya,[2] Tadayoshi Miyamoto,[2,3] Shuji Shimizu,[2] Toshiaki Shishido,[2] Scott A. Smith,[1] and Masaru Sugimachi[2]

[1]*Departments of Physical Therapy and Internal Medicine, University of Texas Southwestern Medical Center at Dallas, Dallas, Texas;* [2]*Department of Cardiovascular Dynamics, National Cerebral and Cardiovascular Center Research Institute, Osaka, Japan; and* [3]*Department of Physical Therapy, Morinomiya University of Medical Sciences, Osaka, Japan*

Submitted 23 November 2010; accepted in final form 26 January 2011

Mizuno M, Kawada T, Kamiya A, Miyamoto T, Shimizu S, Shishido T, Smith SA, Sugimachi M. Exercise training augments the dynamic heart rate response to vagal but not sympathetic stimulation in rats. *Am J Physiol Regul Integr Comp Physiol* 300: R969–R977, 2011. First published January 26, 2011; doi:10.1152/ajpregu.00768.2010.—We examined the transfer function of autonomic heart rate (HR) control in anesthetized sedentary and exercise-trained (16 wk, treadmill for 1 h, 5 times/wk at 15 m/min and 15-degree grade) rats for comparison to HR variability assessed in the conscious resting state. The transfer function from sympathetic stimulation to HR response was similar between groups (gain, 4.2 ± 1.5 vs. 4.5 ± 1.5 beats·min^{-1}·Hz^{-1}; natural frequency, 0.07 ± 0.01 vs. 0.08 ± 0.01 Hz; damping coefficient, 1.96 ± 0.55 vs. 1.69 ± 0.15; and lag time, 0.7 ± 0.1 vs. 0.6 ± 0.1 s; sedentary vs. exercise trained, respectively, means ± SD). The transfer gain from vagal stimulation to HR response was 6.1 ± 3.0 in the sedentary and 9.7 ± 5.1 beats·min^{-1}·Hz^{-1} in the exercise-trained group ($P = 0.06$). The corner frequency (0.11 ± 0.05 vs. 0.17 ± 0.09 Hz) and lag time (0.1 ± 0.1 vs. 0.2 ± 0.1 s) did not differ between groups. When the sympathetic transfer gain was averaged for very-low-frequency and low-frequency bands, no significant group effect was observed. In contrast, when the vagal transfer gain was averaged for very-low-frequency, low-frequency, and high-frequency bands, exercise training produced a significant group effect ($P < 0.05$ by two-way, repeated-measures ANOVA). These findings suggest that, in the frequency domain, exercise training augments the dynamic HR response to vagal stimulation but not sympathetic stimulation, regardless of the frequency bands.

heart rate variability; transfer function; systems analysis

HEART RATE VARIABILITY (HRV) is considered to be a useful noninvasive assessment of autonomic nervous system activity. It has been well recognized that exercise training increases HRV at rest (4, 19). A recent meta-analysis by Sandercock et al. (28) demonstrated that exercise training results in significant increases in R-R interval and high-frequency (HF) power of HRV. Nevertheless, not all studies have demonstrated increases in HRV after exercise training (7). To date, the exact mechanisms underlying increases in HRV after exercise training remain to be elucidated. Many earlier studies have suggested that the augmentation of HRV induced by exercise training may be caused by a withdrawal of sympathetic tonus and/or an increase in vagal tonus (5, 14, 36). Autonomic tone assessed by HRV may reflect both the autonomic outflow from the central nervous system and the peripheral autonomic regulation of atrial pacemaker cells. The latter can be assessed quantitatively by examining the heart rate (HR) response to electrical stimulation of the autonomic nerves. Furthermore, recent studies suggested that peripheral autonomic regulation of atrial pacemaker cells could contribute to the exercise training-induced increases in cardiac vagal function (9, 10).

Equivocal results, however, have been reported using autonomic nerve stimulation. Regarding the vagal system, the effects of exercise training have been inconsistent among studies, showing both increases (9, 10) and reductions in vagally stimulated HR control (25). When considering the sympathetic system, a previous study demonstrated that the HR response to sympathetic stimulation was reduced by exercise training (22). However, the mechanisms underlying the training effect are controversial (3, 15, 26, 29, 33, 35). These equivocal results could be explained by differences in species and modes of exercise training among studies (i.e., exercise type, intensity, and duration, etc.). More importantly, since these studies of autonomic nerve stimulation did not evaluate HRV, a causal relationship between increased HRV and adaptation in peripheral autonomic HR control remains largely undetermined. Furthermore, despite the fact that HRV has been evaluated by using frequency domain as well as time domain analyses, to date, there are no reports available examining the effects of exercise training on the dynamic HR response to sympathetic or vagal stimulation in the frequency domain. Analysis of peripheral autonomic regulation in the frequency domain would advance our understanding of the mechanisms responsible for the alterations in HRV that occur in response to exercise training.

We have recently developed a technique to assess the dynamic characteristics of HR control by the autonomic nervous system in rats using transfer function analysis (21). The transfer function analysis can quantitatively evaluate the HR response to autonomic nerve stimulation over a wide frequency range that is necessary for interpreting the generation of HRV. Therefore, the aims of the present study were *1*) to identify the dynamic characteristics of sympathetic and vagal HR control in exercised-trained rats and *2*) to determine whether alterations in peripheral autonomic regulation contribute to changes in the frequency components of HRV in exercised-trained rats.

MATERIALS AND METHODS

Animal Care and Training Program

Animal care was in accordance with the "Guiding Principles for Care and Use of Animals in the Field of Physiological Sciences," approved by the Physiological Society of Japan. All protocols were reviewed and approved by the Animal Subjects Committee of the

Address for reprint requests and other correspondence: M. Mizuno, Dept. of Physical Therapy, Univ. of Texas Southwestern Medical Center at Dallas, 5323 Harry Hines Blvd., Dallas, TX 75390-9174 (e-mail: masaki.mizuno@utsouthwestern.edu).

National Cerebral and Cardiovascular Center. Fourteen male Sprague-Dawley rats (200–250 g body wt) were fed standard laboratory chow and water ad libitum and housed three per cage in a temperature-controlled room with a 12:12-h dark-light cycle. Rats were randomly assigned to one of two groups: sedentary ($n = 7$) and exercise trained ($n = 7$).

Exercise training was performed on a motor-driven treadmill, 5 days/wk for 16 wk, gradually progressing toward a speed of 15 m/min at a 15-degree grade for 60 min. Sedentary rats walked (10 m/min at 15 degrees) 10 min/day once per week during the 16-wk period to maintain treadmill familiarity. At the end of the 16-wk period, maximal exercise capacity was measured twice in each rat in tests separated by 2 days (6). The protocol for the maximal exercise capacity test consisted of walking at 10 m/min for 5 min followed by 2 m/min increases in speed every 2 min until the rat reached exhaustion. Rats were considered exhausted when they failed to stay off of a shock bar.

Assessment of Autonomic Tone in the Conscious Resting State

After the performance test, three steel electrodes were implanted under anesthesia. These electrodes were utilized for monitoring the electrocardiogram. The R-R interval was measured using a cardiotachometer (model AT601G; Nihon Kohden, Tokyo, Japan). On the first day of the study, which was 24 h after electrodes had been implanted, resting HR was recorded to analyze the R-R interval variability in the quiet unrestrained rat that was kept in a small box. In accordance with a previous study (25), autonomic tone was assessed by intraperitoneal injections of methylatropine (3 mg/kg) and propranolol (4 mg/kg). Immediately after resting HR was recorded, methylatropine was injected. Since the HR response to methylatropine reached its peak in 10–15 min, this time interval was allocated before the HR measurement. Propranolol was injected after methylatropine injection, and again the HR was measured after 10–15 min. Intrinsic HR was evaluated after simultaneous blockade by propranolol and methylatropine. Sympathetic tonus was defined as the difference between the HR after methylatropine injection and intrinsic HR. On the second day, propranolol was administered first to obtain the inverse sequence of blockade. Vagal tonus was defined as the difference between the HR after propranolol injection and intrinsic HR.

Sympathetic and Vagal Stimulation

Surgical preparations. After obtaining data for the assessment of autonomic tone and HRV, rats were anesthetized by a mixture of urethane (250 mg/ml) and α-chloralose (40 mg/ml), initiated with an intraperitoneal bolus injection of 1 ml/kg. If additional anesthesia was needed, 0.1 ml/kg was given intraperitoneally. The rats were intubated and mechanically ventilated with oxygen-enriched room air. The rats were slightly hyperventilated to suppress chemoreflexes. A catheter was placed in the right femoral artery and connected to a pressure transducer (model DX-200; Nihon Kohden, Tokyo, Japan) to measure arterial pressure (AP). HR was measured using a cardiotachometer (model AT601G; Nihon Kohden) triggered by the R wave on the electrocardiogram. A catheter was introduced into the right femoral vein for drug administration. Sinoaortic barodenervation was performed bilaterally to minimize changes in sympathetic efferent nerve activity via arterial baroreflexes. The vagi were sectioned bilaterally at the neck. A pair of bipolar stainless steel electrodes was attached to the right cervical sympathetic nerve for efferent sympathetic stimulation or the right cervical vagus for efferent vagal stimulation. The stimulation electrodes and nerve were secured with silicon glue (Kwik-Sil; World Precision Instruments, Sarasota, FL). Body temperature was monitored with a thermometer placed in the rectum and was maintained at 38°C with a heating pad throughout the experiment.

Experimental procedures. The pulse duration was set at 2 ms and the stimulation amplitude was fixed at 10 V for both sympathetic and vagal nerve stimulation. To allow for stabilization of hemodynamics, sympathetic and vagal nerve stimulations were started ~1 h after the end of surgical preparations. Between sympathetic and vagal stimulation protocols > 15 min elapsed to allow AP and HR to return to their respective baseline values.

To estimate the dynamic transfer characteristics from sympathetic stimulation to HR response, the sectioned end of the right cervical sympathetic nerve was stimulated employing a frequency-modulated pulse train for 10 min. The stimulation frequency was switched every 1,000 ms to either 0 or 5 Hz according to a binary white noise signal. The power spectrum of the stimulation signal was reasonably constant up to 0.5 Hz. The transfer function was estimated up to 0.5 Hz because the reliability of estimation decreased due to the diminution of input power above this frequency. The selected frequency range sufficiently spanned the range of physiological interest (21). For estimation of the static transfer characteristics from sympathetic stimulation to HR response, stepwise sympathetic stimulation was performed. Sympathetic stimulation frequency was increased from 1 to 5 Hz in 1-Hz increments. Each frequency step was maintained for 60 s.

To estimate the dynamic transfer characteristics from vagal stimulation to HR response, the right vagus was stimulated employing a frequency-modulated pulse train for 10 min. The stimulation frequency was switched every 500 ms to either 0 or 10 Hz according to a binary white noise signal. The power spectrum of the stimulation signal was reasonably constant up to 1 Hz. The transfer function was estimated up to 1 Hz because the reliability of estimation decreased due to the diminution of input power above this frequency. The selected frequency range sufficiently spanned the range of physiological interest (21). For estimation of the static transfer characteristics from vagal stimulation to HR response, stepwise vagal stimulation was performed. Vagal stimulation frequency was changed among 2, 4, 8, 16, and 32 Hz. Each frequency step was maintained for 60 s.

Data Analysis

Spectral analysis of HRV. Data obtained during the conscious resting state were digitized at 200 Hz utilizing a 12-bit analog-to-digital converter and stored on the hard disk of a dedicated laboratory computer system. Beat-by-beat time series of the R-R interval were interpolated every 130 ms (Δt). Twelve data segments of 512 (N) points overlapping half of the preceding data were processed. For each data segment, after the linear trend was removed and the Hanning window applied, power spectral density was computed using the fast Fourier transform algorithm. The frequency resolution was $\Delta f = 1/(N\,\Delta t)$, i.e., 0.015 Hz, and the highest frequency was $\Delta f = 1/2\Delta t$, i.e., 3.85 Hz, where f is frequency. The very-low-frequency (VLF) band ranged between 0.017 and 0.27 Hz, the low-frequency (LF) band between 0.27 and 0.75 Hz, and the high-frequency (HF) band between 0.75 and 3.3 Hz, according to an earlier report (8). The percentage of LF or HF power relative to the sum of LF and HF powers and the ratio of LF to HF power were also calculated.

Transfer function analysis. The dynamic characteristics of the HR response to sympathetic or vagal stimulation were estimated by a transfer function analysis (see APPENDIX for details). Dynamic sympathetic control of HR was quantified by fitting a second-order low-pass filter with pure delay to the estimated transfer function. The dynamic vagal control of HR was quantified by fitting a first-order, low-pass filter with pure delay to the estimated transfer function. To facilitate the intuitive understanding of the system's dynamic characteristics, we calculated the system step response of HR to 1-Hz nerve stimulation as follows.

The system impulse response was derived from the inverse Fourier transform of the transfer function. The system step response was then obtained from the time integral of the impulse response. The length of the step response was 51.2 s. The 80% rise time for the sympathetic step response or the 80% fall time for the vagal step response was estimated as the time at which the step response reached 80% of the

Table 1. *Physical characteristics*

	Sedentary	Exercise Trained
Body weight, g	642 ± 33	534 ± 33*
Ventricular weight, g	1.22 ± 0.03	1.17 ± 0.04*
Ventricular weight/body weight, g/kg	1.9 ± 0.1	2.2 ± 0.1*
Lung weight, g	2.13 ± 0.27	1.89 ± 0.38
Lung weight/body weight, g/kg	3.3 ± 0.3	3.5 ± 0.7
Performance test, s	1150 ± 165	1790 ± 389*

Values are means ± SD. *$P < 0.05$ compared with sedentary group.

steady-state response calculated by averaging the last 10 s of data of the step response.

Statistical Analysis

All data are represented as means ± SD. Data were analyzed using unpaired Student's *t*-tests (sedentary vs. exercise trained) or two-way, repeated-measures ANOVA. Values of $P < 0.05$ were considered to be significant.

RESULTS

Physical Characteristic

Morphometric characteristics and exercise capacity for sedentary and exercised-trained rats are presented in Table 1. The mean body weight of the exercised-trained rats was significantly smaller than that of the sedentary rats. The mean ventricular weight of the exercised-trained rats was slightly but significantly smaller than that of the sedentary rats. Consequently, the ventricular weight normalized by body weight was significantly greater in the exercised-trained compared with the sedentary group. The lung weight-to-body weight ratio was not different between the groups. Exercise capacity was 64% greater in the exercised-trained than in the sedentary group. The reproducibility of measuring the maximal exercise capacity was reasonably high ($y = 1.2x - 226.1$, $R^2 = 0.79$; x and y represent the first and second measurements).

Spectral Analysis of HRV and Autonomic Tone in the Conscious Resting State

The power spectral densities of R-R interval are shown in Table 2. The percentage of LF power was significantly smaller, and the percentage of HF power was significantly greater in the exercised-trained rats than in the sedentary rats. The LF/HF ratio in the exercised-trained rats was significantly smaller compared with that in the sedentary rats. HR at rest was significantly lower in the exercised-trained compared with the sedentary group (Fig. 1*A*). The intrinsic HR was similar between the groups (Fig. 1*A*). Although the sympathetic tonus was comparable between the groups, the vagal tonus tended to be greater ($P = 0.08$) in the exercised-trained compared with the sedentary group (Fig. 1*B*).

Dynamic Sympathetic and Vagal Transfer Functions

Table 3 summarizes hemodynamics during dynamic sympathetic stimulation. Sympathetic stimulation significantly increased mean HR in both sedentary and exercised-trained groups. Mean HR and AP did not differ between the groups, before and during sympathetic stimulation. Figure 2*A* illustrates the dynamic transfer function characterizing sympathetic HR control. The frequency band effect was significant ($P < 0.0001$) but the group effect was insignificant ($P = 0.5461$) in the dynamic gain values of the sympathetic transfer function by two-way, repeated-measures ANOVA. The parameters of the sympathetic transfer function were comparable between the groups (Table 4). Figure 2*B* shows the calculated step response of HR to sympathetic stimulation. The steady-state response and the 80% rise time did not differ significantly between the groups (Table 4).

Table 5 summarizes hemodynamics during dynamic vagal stimulation. Vagal stimulation significantly decreased mean HR in both sedentary and exercised-trained groups. Mean HR and AP did not differ between the groups, before and during vagal stimulation. Figure 3*A* illustrates the dynamic transfer function characterizing vagal HR control. The frequency band effect ($P < 0.0001$) and the group effect ($P < 0.0001$) were both significant in the dynamic gain values of the vagal transfer function by two-way, repeated-measures ANOVA. The estimated dynamic gain (*see* APPENDIX) tended to be greater in the exercised-trained compared with the sedentary group ($P = 0.06$, Table 6). Other parameters did not differ between the groups. Figure 3*B* shows the calculated step response of HR to vagal stimulation. The calculated steady-state response in the exercised-trained rats also tended to be greater than that in the sedentary rats ($P = 0.06$, Table 6). There was no significant difference in the 80% fall time between the groups.

Dynamic Gain Values of Sympathetic and Vagal Transfer Function Corresponding to HRV Frequency Bands

When dynamic gain values of the sympathetic transfer function were averaged for the VLF and LF (up to 0.5 Hz, see METHODS) bands, the frequency band effect was significant, but the group effect was insignificant by two-way, repeated-measures ANOVA (Fig. 4*A*). When dynamic gain values of the vagal transfer function were averaged for the VLF, LF, and HF (up to 1 Hz, see METHODS) bands, the frequency band effect was insignificant but the group effect was significant such that the dynamic gain was significantly greater in the exercised-trained compared with the sedentary group (Fig. 4*B*).

Static Sympathetic and Vagal Transfer Function

The increase in HR with stepwise sympathetic stimulation was similar between groups (Fig. 5*A*). The stimulation frequency effect was significant, while the group effect was insignificant by two-way, repeated-measures ANOVA. In contrast, the decrease in HR with stepwise vagal stimulation was greater in the exercised-trained compared with sedentary rats (Fig. 5*B*). Both the stimulation frequency effect and the group effect were significant.

Table 2. *Spectral parameters of R-R interval*

	Sedentary	Exercise Trained
Variance, ms^2	87 ± 39	90 ± 32
VLF, ms^2	73 ± 30	80 ± 30
LF, ms^2	6.3 ± 3.4	3.1 ± 3.0
LF, %	49 ± 11	36 ± 7*
HF, ms^2	8.0 ± 7.6	6.2 ± 7.1
HF, %	51 ± 11	64 ± 7*
LF/HF ratio	1.0 ± 0.5	0.6 ± 0.2*

Values are means ± SD. LF, low frequency; VLF, very low frequency; HF, high frequency; *$P < 0.05$ compared with sedentary group.

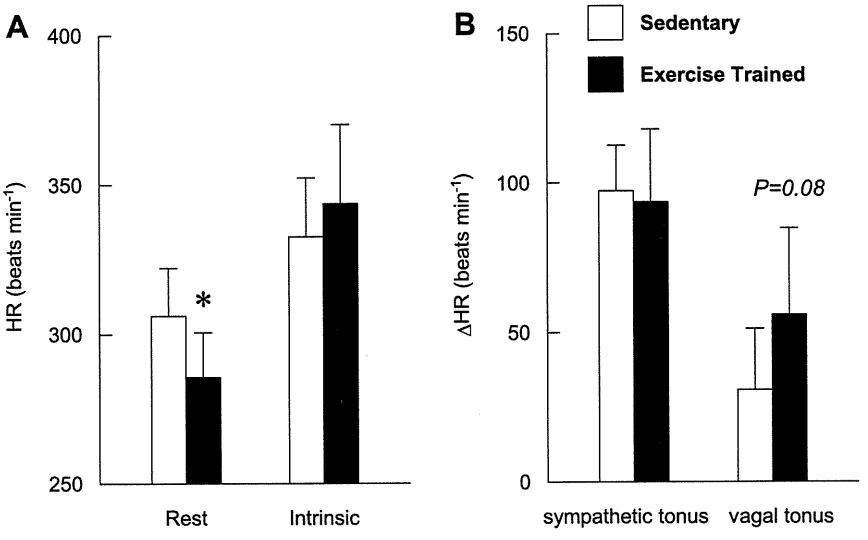

Fig. 1. Heart rate (HR) at rest and intrinsic HR (*A*) and HR sympathetic and vagal tone (*B*) obtained in sedentary and exercised-trained rats. *$P < 0.05$ compared with sedentary group.

DISCUSSION

We have examined the dynamic transfer function of autonomic HR control by using random binary sympathetic and vagal nerve stimulation in sedentary and exercised-trained rats. The major findings in the present study are *1*) that the exercise training did not alter the sympathetic transfer function substantially but augmented the dynamic gain of the vagal transfer function; and *2*) in the frequency domain, exercise training increased the dynamic HR response to vagal stimulation but not sympathetic stimulation, regardless of the frequency band. These findings are the first quantitative data on the effect of exercise training on the dynamic characteristics of peripheral HR control by the sympathetic and vagal systems.

Validity of Exercise Training

The relative ventricular hypertrophy and higher exercise capacity in the exercised-trained compared with the sedentary group suggested that exercise program used in the present study was sufficient to induce physiological adaptations commensurate with an effective training stimulus. As is well known, exercise training induces bradycardia at rest (Fig. 1*A*). Moreover, changes in the spectral parameters for R-R interval (Table 2) and autonomic tone (Fig. 1*B*) induced by the exercise training are consistent with earlier studies in rats (30, 31).

Effect of Exercise Training on Sympathetic and Vagal Transfer Function

Exercise training altered neither dynamic (Fig. 2) nor static sympathetic transfer function (Fig. 5*A*). These results are different than those reported in a previous study in which swim training significantly reduced the HR response to sympathetic nerve stimulation in a double atrial/right stellate ganglion preparation in guinea pigs (22). The discrepancy between investigations may have arisen from differences in the nerves experimentally stimulated (cervical sympathetic nerve vs. stellate ganglion), animal species studied (rats vs. guinea pigs), and/or experimental preparation utilized (in vivo vs. ex vivo). The mechanisms underlying the sympathetically mediated exercise training effect on HR are also controversial. For instance, chronotropic responsiveness to isoproterenol has been reported to be decreased in one study (15) but unchanged in another (22) by exercise training. Furthermore, in response to exercise training, the density and affinity of β-adrenoceptors in the heart have been shown to be reduced in some reports (26, 33), while unchanged in others (3, 34, 35).

Table 3. *Arterial pressure(AP) and heart rate (HR) during dynamic sympathetic stimulation protocol*

	Sedentary		Exercise Trained	
	Prestimulation	During Stimulation	Prestimulation	During Stimulation
AP, mmHg	74 ± 16	68 ± 15†	89 ± 17	84 ± 24
HR, beats/min	377 ± 25	444 ± 23†	381 ± 16	444 ± 26†

Values are means ± SD. †$P < 0.05$ compared with prestimulation.

Exercise training augmented the dynamic gain of the vagal transfer function (Fig. 2). The effect of exercise training was also significant for static vagal transfer function (Fig. 5*B*). These results are in agreement with previous studies showing that exercise training significantly augmented the HR response to vagal nerve stimulation in a double atrial/right vagal nerve preparation using mice (9, 10). In contrast, Negrao et al. (25) demonstrated that the HR response to vagal stimulation was depressed in exercised-trained rats. A possible explanation for this disparate result is that the arterial baroreflexes remained intact in the experimental preparation used in the study (25). In contrast, sinoaortic barodenervation was performed in the present investigation to minimize baroreflex-mediated changes in sympathetic efferent nerve activity. Exercise training has been shown to attenuate the baroreflex-mediated sympathetic nerve response to hypotension (11). Although speculative, in the study by Negrao et al. (25), baroreflex-mediated sympathetic activation in response to vagally-induced hypotension might have been less in exercised-trained compared with sedentary rats. Consequently, the gain of vagal stimulation might have been attenuated in exercised-trained animals relative to sedentary rats. This suggestion is reasonable given that accentuated antagonism is indicative of a diminution in background sym-

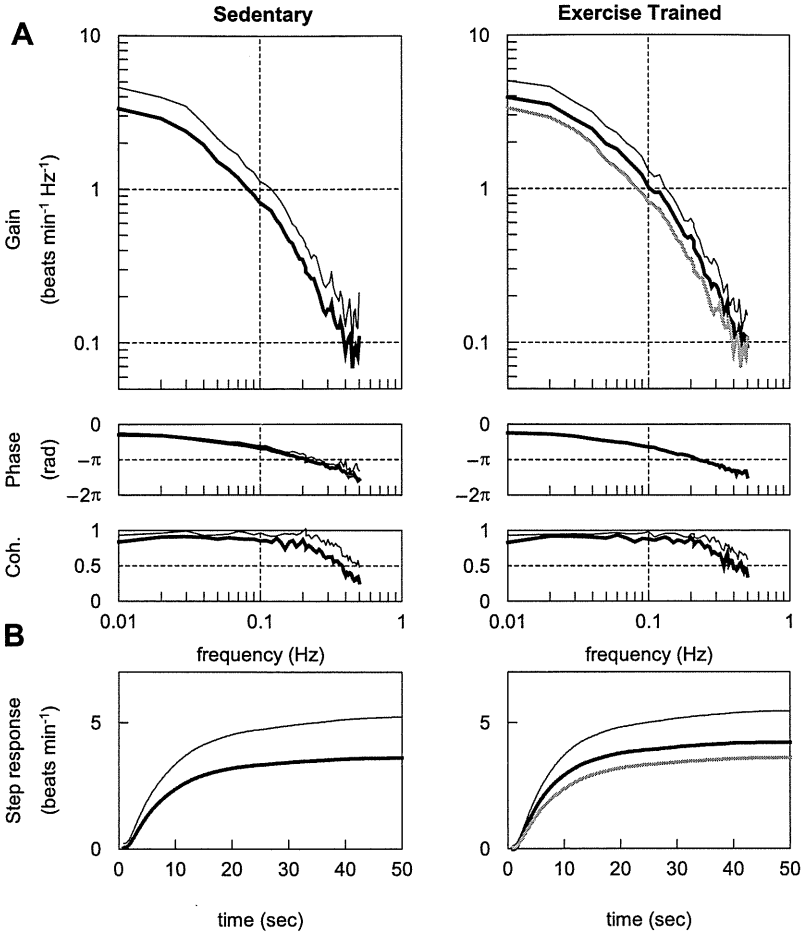

Fig. 2. *A*: transfer function from sympathetic stimulation to the HR response obtained in sedentary and exercised-trained rats. Gains (*top*), phase shifts (*middle*), and coherence (Coh.) functions (*bottom*) are presented. *B*: calculated step response to 1-Hz tonic sympathetic stimulation. Thick lines represent the mean, whereas thin lines indicate ± SD values. The gray solid curves in the gain and step response panels (*right*) duplicates the means (*left*).

pathetic tonus, which can decrease the gain of the vagal transfer function (17).

It has been documented that the intensity of exercise as well as the duration of exercise training are related to the autonomic adaptation to exercise training (28). These factors have been shown to be largely variable among different studies. A well-controlled experimental setup is needed to clarify these issues.

Dynamic Gain Values of Sympathetic and Vagal Transfer Functions Corresponding to HRV Frequency Bands

HRV is considered to reflect autonomic tone (19). The VLF component is likely to reflect changes in vasomotor tone in relation to thermoregulation and local adjustment of resistance in individual vascular beds; the LF component is considered to be a marker of sympathetic activity, although it remains a matter of debate; and the HF component mainly originates from respiratory activity and is considered to be mediated by vagal input (27). In rats, Cerutti et al. (8) determined that the LF component ranged between 0.27 and 0.74 Hz, and the HF component was > 0.75 Hz.

Averaged dynamic gain values of sympathetic transfer function for VLF and LF bands did not differ between the sedentary and exercised-trained groups (Fig. 4*A*). These results suggest that changes in the peripheral sympathetic control of HR likely do not contribute significantly to training-induced alterations in HRV. Therefore, the lower percentage of LF power and LF/HF ratio in the exercised-trained group (Table 2) may indicate reduced activation of sympathetic outflow from autonomic centers (23). In contrast, averaged dynamic gain values of vagal transfer function for VLF, LF, and HF bands (Fig. 4*B*) as

Table 4. *Sympathetic transfer function parameters and step response*

	Sedentary	Exercise Trained
Gain, beats·min^{-1}·Hz^{-1}	4.2 ± 1.5	4.5 ± 1.5
Natural frequency, Hz	0.07 ± 0.01	0.08 ± 0.01
Damping ratio	1.96 ± 0.55	1.69 ± 0.15
Lag time, s	0.71 ± 0.10	0.62 ± 0.11
Steady-state response, beats/min	3.6 ± 1.6	4.2 ± 1.2
80% rise time, s	12.9 ± 2.7	12.1 ± 3.0

Values are means ± SD. See APPENDIX for transfer function parameters.

Table 5. *AP and HR during dynamic vagal stimulation protocol*

	Sedentary		Exercise Trained	
	Prestimulation	During stimulation	Prestimulation	During stimulation
AP, mmHg	72 ± 21	68 ± 15	92 ± 14	80 ± 21
HR, beats/min	373 ± 18	327 ± 38 †	372 ± 14	301 ± 32 †

Values are means ± SD. †$P < 0.05$ compared with prestimulation.

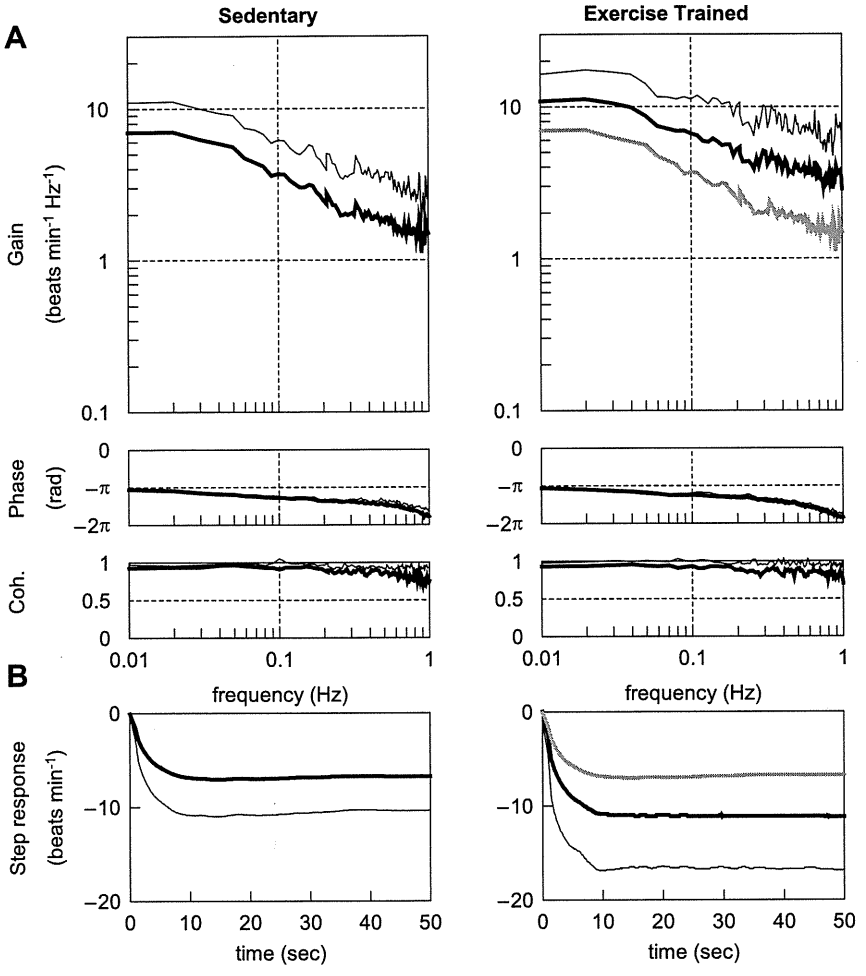

Fig. 3. *A*: transfer function from vagal stimulation to the HR response obtained in sedentary and exercised-trained rats. Gains (*top*), phase shifts (*middle*), and coherence functions (*bottom*) are presented. *B*: calculated step response to 1-Hz tonic vagal stimulation. Thick lines represent the mean, whereas thin lines indicate ± SD values. The gray solid curves in the gain and step response panels (*right*) duplicate the means (*left*).

well as the percentage of HF power (Table 2) were significantly greater in the exercised-trained compared with the sedentary group. These results suggest that the augmentation in HRV induced by exercise training is, at least in part, mediated by augmentations in the peripheral vagal control of HR.

What are the possible mechanisms underlying augmentations in the peripheral vagal control of HR? Danson and Paterson (10) have presented evidence that neuronal nitric oxide synthase may be a key enzymatic protein underlying such training-induced increases in cardiac vagal function. This group has also demonstrated that HR changes in response to vagal stimulation are enhanced by exercise training in wild-type mice but not in heterozygous neuronal nitric oxide synthase knockout mice (9). Another candidate for augmentations in the peripheral vagal control of HR is muscarinic receptors, which play a fundamental role in HR control via vagally mediated regulation. However, the effects of exercise training have been inconsistent among studies, showing both increases (12) and no change (2, 3) in muscarinic receptors in the myocardium of rats. The possibility cannot be dismissed that training-induced changes in the activity of afferent inputs mediating vagal outflow may also contribute to the alterations in HRV (4). Further investigation is needed to clarify these issues.

Table 6. *Vagal transfer function parameters and step response*

	Sedentary	Exercise Trained
Gain, beats·min^{-1}·Hz^{-1}	6.1 ± 3.0	9.7 ± 5.1#
Corner frequency, Hz	0.11 ± 0.05	0.17 ± 0.09
Lag time, s	0.10 ± 0.08	0.17 ± 0.08
Steady-state response, beats/min	−6.7 ± 3.6	−11.2 ± 5.7#
80% Fall time, s	4.3 ± 2.2	4.3 ± 1.5

Values are means ± SD. #P = 0.06 compared with sedentary group. See APPENDIX for transfer function parameters.

Perspectives and Significance

To date, the mechanisms underlying increased HRV after exercise training remain to be elucidated. HRV may reflect both the autonomic outflow from the central nervous system and the peripheral autonomic regulation of atrial pacemaker cells. In human studies, it is difficult to separately examine each factor. The findings of the present study suggest that the augmentation in HRV induced by exercise training is, at least in part, mediated by augmentations in the peripheral vagal control of HR. In other words, even if vagal outflow from the central nervous system remains unchanged after exercise training, HRV could be increased by an enhanced responsiveness in the peripheral vagal, but not sympathetic, regulation of HR.

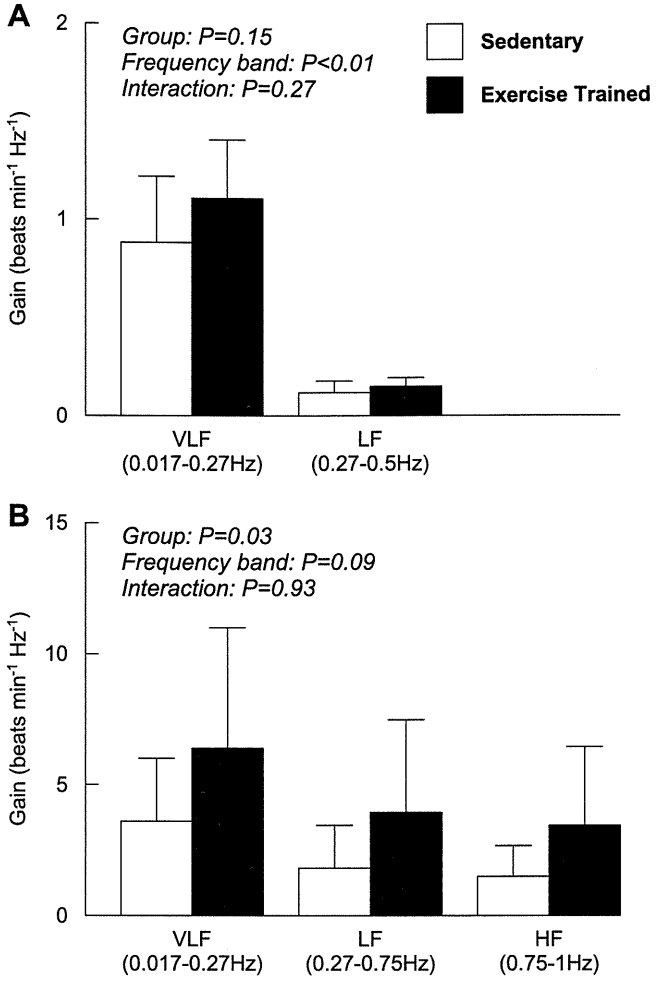

Fig. 4. Averaged sympathetic (*A*) and vagal (*B*) gain calculated from corresponding transfer function in very low frequency (VLF), low frequency (LF), and high frequency (HF) bands.

It has been well documented that decreased HRV is observed in heart failure (18) as well as in a variety of lifestyle-related diseases such as diabetes (16), hypertension (24), and obesity (1). Furthermore, reductions in HRV are related to increases in mortality rates as well as the occurrence of adverse cardiac events (32). Exercise training-induced augmentations in HRV maintain the potential to partially correct or normalize the autonomic dysfunction manifest in these disease states (4). Understanding the mechanisms contributing to the alterations in HRV induced by exercise training may significantly impact the development of novel therapeutic strategies for the treatment of autonomic dysfunction.

Limitations

There are several limitations to this study. First, the rats were slightly hyperventilated throughout the stimulation protocol. We cannot rule out the possibility that the hyperventilation might have affected the results reported. Second, dynamic sympathetic stimulation lowered mean AP in sedentary rats although sinoaortic barodenervation was performed. This may be explained by a possible difference in left ventricular functional capacity. For example, under conditions of equivalent HR, changes in systolic blood pressure were smaller in sedentary rats compared with exercised-trained rats (13). Third, the stimulation amplitude was fixed at 10 V for both sympathetic and vagal nerve stimulation. It should be noted, however, that our preliminary results indicated that 10 V was sufficiently large enough to evoke maximal HR responses. Fourth, transfer function data were obtained from anesthetized animals. This must be taken into account when interpreting the present results as anesthesia may affect the peripheral autonomic regulation of atrial pacemaker cells. Finally, we stimulated the sympathetic and vagal nerves according to a binary white noise signal. Although this method of stimulation is quite different from the physiological pattern of neuronal discharge, the coherence was near unity over the frequency range of interest. This finding indicates that the system properties do not vary considerably in response to different patterns of stimulation.

Conclusion

In the present study, it was demonstrated for the first time that exercise training did not alter dynamic sympathetic control of HR, while it did augment dynamic vagal control of HR. In addition, the group effect was significant with regard to the dynamic gain values for the vagal transfer functions corresponding to VLF, LF, and HF bands. This finding suggests that enhancements in the peripheral vagal control of HR may, at

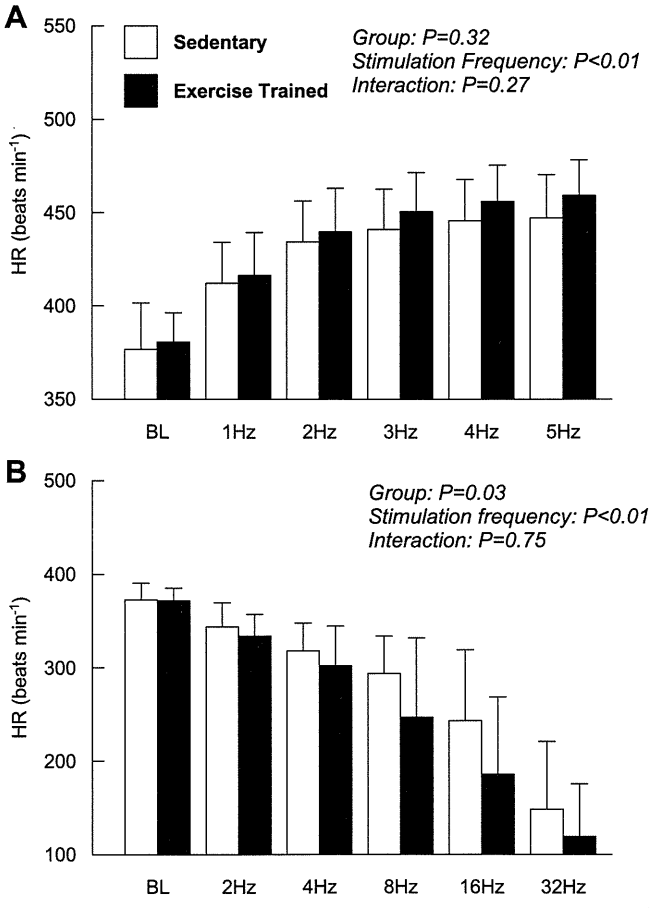

Fig. 5. HR response to stepwise sympathetic (*A*) and vagal (*B*) stimulation obtained in sedentary and exercised-trained rats.

least in part, contribute to the exercise-induced augmentation in HRV in healthy rats.

APPENDIX: TRANSFER FUNCTION ANALYSIS

The dynamic transfer function from binary white noise stimulation to the HR response was estimated based on the following procedure. Input-output data pairs of the stimulation frequency and HR were resampled at 10 Hz to be consistent with our previous study (21). Subsequently, data pairs were partitioned into eight 50% overlapping segments consisting of 1,024 data points each. For each segment, the linear trend was subtracted and a Hanning window was applied. A fast Fourier transform was then performed to obtain the frequency spectra of nerve stimulation [$N(f)$] and HR [$HR(f)$]. Over the eight segments, the power of the nerve stimulation [$S_{N\cdot N}(f)$], the power of the HR [$S_{HR\cdot HR}(f)$], and the cross-power between these two signals [$S_{N\cdot HR}(f)$] were ensemble averaged. Finally, the transfer function [$H(f)$] from nerve stimulation to the HR response was determined using the following equation (20).

$$H(f) = \frac{S_{N\text{-}HR}(f)}{S_{N\cdot N}(f)}$$

To quantify the linear dependence of the HR response on vagal or sympathetic stimulation, the magnitude-squared coherence function [Coh(f)] was estimated employing the following equation (20).

$$\mathrm{Coh}(f) = \frac{|S_{\mathrm{N\text{-}HR}}(f)|^2}{S_{\mathrm{N\cdot N}}(f) \cdot S_{\mathrm{HR\cdot HR}}(f)}$$

Coherence values range from zero to unity. Unity coherence indicates perfect linear dependence between the input and output signals; in contrast, zero coherence indicates total independence between the two signals.

Since the transfer function from sympathetic stimulation to HR response in rats approximated a second order low-pass filter with pure delay (21), we determined the parameters of the sympathetic transfer function using the following equation.

$$H(f) = \frac{K}{1 + 2\zeta\frac{f}{f_N}j + \left(\frac{f}{f_N}j\right)^2} e^{-2\pi f j L}$$

where K is dynamic gain (in beats·min^{-1}·Hz^{-1}), f_N is the natural frequency (in Hz), ζ is the damping ratio, L is lag time (in s), and f and j represent frequency and imaginary units, respectively. These parameters were estimated by means of an iterative nonlinear least squares regression.

Since the transfer function from vagal stimulation to HR response in rats approximated a first-order, low-pass filter with pure delay (21), we determined the parameters of the vagal transfer function using the following equation.

$$H(f) = \frac{-K}{1 + \frac{f}{f_C}j} e^{-2\pi f j L}$$

where K represents the dynamic gain (in beats·min^{-1}·Hz^{-1}), fc denotes the corner frequency (in Hz), L denotes the lag time (in s), and f and j represent frequency and imaginary units, respectively. The negative sign in the numerator indicates the negative HR response to vagal stimulation. These parameters were estimated by means of an iterative nonlinear least squares regression.

GRANTS

This study was supported by Health and Labor Sciences Research Grants H18-nano-Ippan-003, H19-nano-Ippan-009, H20-katsudo-Shitei-007, and H21-nano-Ippan-005 from the Ministry of Health, Labor and Welfare of Japan, by Grants-in-Aid for Scientific Research No. 19700559 from the Ministry of Education, Culture, Sports, Science and Technology in Japan, and by the Industrial Technology Research Grant Program from New Energy and Industrial Technology Development Organization of Japan. M. Mizuno was supported from Research Fellowships of the Japan Society for the Promotion of Science for Young Scientists.

DISCLOSURES

No conflicts of interest, financial or otherwise, are declared by the author(s).

REFERENCES

1. **Arone LJ, Mackintosh R, Rosenbaum M, Leibel RL, Hirsch J.** Autonomic nervous system activity in weight gain and weight loss. *Am J Physiol Regul Integr Comp Physiol* 269: R222–R225, 1995.
2. **Barbier J, Rannou-Bekono F, Marchais J, Berthon PM, Delamarche P, Carre F.** Effect of training on β1-, β2-, β3-adrenergic and M2 muscarinic receptors in rat heart. *Med Sci Sports Exerc* 36: 949–954, 2004.
3. **Barbier J, Reland S, Ville N, Rannou-Bekono F, Wong S, Carre F.** The effects of exercise training on myocardial adrenergic and muscarinic receptors. *Clin Auton Res* 16: 61–65, 2006.
4. **Billman GE.** Cardiac autonomic neural remodeling and susceptibility to sudden cardiac death: effect of endurance exercise training. *Am J Physiol Heart Circ Physiol* 297: H1171–H1193, 2009.
5. **Blomqvist CG, Saltin B.** Cardiovascular adaptations to physical training. *Annu Rev Physiol* 45: 169–189, 1983.
6. **Brenner DA, Apstein CS, Saupe KW.** Exercise training attenuates age-associated diastolic dysfunction in rats. *Circulation* 104: 221–226, 2001.
7. **Buch AN, Coote JH, Townend JN.** Mortality, cardiac vagal control and physical training–what's the link? *Exp Physiol* 87: 423–435, 2002.
8. **Cerutti C, Gustin MP, Paultre CZ, Lo M, Julien C, Vincent M, Sassard J.** Autonomic nervous system and cardiovascular variability in rats: a spectral analysis approach. *Am J Physiol Heart Circ Physiol* 261: H1292–H1299, 1991.
9. **Danson EJ, Mankia KS, Golding S, Dawson T, Everatt L, Cai S, Channon KM, Paterson DJ.** Impaired regulation of neuronal nitric oxide synthase and heart rate during exercise in mice lacking one nNOS allele. *J Physiol* 558: 963–974, 2004.
10. **Danson EJ, Paterson DJ.** Enhanced neuronal nitric oxide synthase expression is central to cardiac vagal phenotype in exercise-trained mice. *J Physiol* 546: 225–232, 2003.
11. **DiCarlo SE, Bishop VS.** Exercise training attenuates baroreflex regulation of nerve activity in rabbits. *Am J Physiol Heart Circ Physiol* 255: H974–H979, 1988.
12. **Favret F, Henderson KK, Clancy RL, Richalet JP, Gonzalez NC.** Exercise training alters the effect of chronic hypoxia on myocardial adrenergic and muscarinic receptor number. *J Appl Physiol* 91: 1283–1288, 2001.
13. **Fitzsimons DP, Bodell PW, Herrick RE, Baldwin KM.** Left ventricular functional capacity in the endurance-trained rodent. *J Appl Physiol* 69: 305–312, 1990.
14. **Goldsmith RL, Bigger JT Jr, Steinman RC, Fleiss JL.** Comparison of 24-hour parasympathetic activity in endurance-trained and untrained young men. *J Am Coll Cardiol* 20: 552–558, 1992.
15. **Hammond HK, White FC, Brunton LL, Longhurst JC.** Association of decreased myocardial β-receptors and chronotropic response to isoproterenol and exercise in pigs following chronic dynamic exercise. *Circ Res* 60: 720–726, 1987.
16. **Ikeda T, Matsubara T, Sato Y, Sakamoto N.** Circadian blood pressure variation in diabetic patients with autonomic neuropathy. *J Hypertens* 11: 581–587, 1993.
17. **Kawada T, Ikeda Y, Sugimachi M, Shishido T, Kawaguchi O, Yamazaki T, Alexander J Jr, Sunagawa K.** Bidirectional augmentation of heart rate regulation by autonomic nervous system in rabbits. *Am J Physiol Heart Circ Physiol* 271: H288–H295, 1996.
18. **La Rovere MT, Pinna GD, Maestri R, Mortara A, Capomolla S, Febo O, Ferrari R, Franchini M, Gnemmi M, Opasich C, Riccardi PG, Traversi E, Cobelli F.** Short-term heart rate variability strongly predicts sudden cardiac death in chronic heart failure patients. *Circulation* 107: 565–570, 2003.

19. **Malliani A, Pagani M, Lombardi F, Cerutti S.** Cardiovascular neural regulation explored in the frequency domain. *Circulation* 84: 482–492, 1991.
20. **Marmarelis P, Marmarelis V.** The white noise method in system identification. In: *Analysis of Physiological Systems*. New York: Plenum, 1978, p. 131–221.
21. **Mizuno M, Kawada T, Kamiya A, Miyamoto T, Shimizu S, Shishido T, Smith SA, Sugimachi M.** Dynamic characteristics of heart rate control by the autonomic nervous system in rats. *Exp Physiol* 95: 919–925, 2010.
22. **Mohan RM, Choate JK, Golding S, Herring N, Casadei B, Paterson DJ.** Peripheral pre-synaptic pathway reduces the heart rate response to sympathetic activation following exercise training: role of NO. *Cardiovasc Res* 47: 90–98, 2000.
23. **Mueller PJ.** Exercise training attenuates increases in lumbar sympathetic nerve activity produced by stimulation of the rostral ventrolateral medulla. *J Appl Physiol* 102: 803–813, 2007.
24. **Mussalo H, Vanninen E, Ikaheimo R, Laitinen T, Laakso M, Lansimies E, Hartikainen J.** Heart rate variability and its determinants in patients with severe or mild essential hypertension. *Clin Physiol* 21: 594–604, 2001.
25. **Negrao CE, Moreira ED, Santos MC, Farah VM, Krieger EM.** Vagal function impairment after exercise training. *J Appl Physiol* 72: 1749–1753, 1992.
26. **Nieto JL, Laviada ID, Guillen A, Haro A.** Adenylyl cyclase system is affected differently by endurance physical training in heart and adipose tissue. *Biochem Pharmacol* 51: 1321–1329, 1996.
27. **Pagani M, Lombardi F, Guzzetti S, Rimoldi O, Furlan R, Pizzinelli P, Sandrone G, Malfatto G, Dell'Orto S, Piccaluga E.** Power spectral analysis of heart rate and arterial pressure variabilities as a marker of sympatho-vagal interaction in man and conscious dog. *Circ Res* 59: 178–193, 1986.
28. **Sandercock GR, Bromley PD, Brodie DA.** Effects of exercise on heart rate variability: inferences from meta-analysis. *Med Sci Sports Exerc* 37: 433–439, 2005.
29. **Schwarz P, Diem R, Dun NJ, Forstermann U.** Endogenous and exogenous nitric oxide inhibits norepinephrine release from rat heart sympathetic nerves. *Circ Res* 77: 841–848, 1995.
30. **Souza SB, Flues K, Paulini J, Mostarda C, Rodrigues B, Souza LE, Irigoyen MC, De Angelis K.** Role of exercise training in cardiovascular autonomic dysfunction and mortality in diabetic ovariectomized rats. *Hypertension* 50: 786–791, 2007.
31. **Tezini GC, Silveira LC, Villa-Cle PG Jr, Jacinto CP, Di Sacco TH, Souza HC.** The effect of aerobic physical training on cardiac autonomic control of rats submitted to ovariectomy. *Menopause* 16: 110–116, 2009.
32. **Tsuji H, Larson MG, Venditti FJ Jr, Manders ES, Evans JC, Feldman CL, Levy D.** Impact of reduced heart rate variability on risk for cardiac events. The Framingham Heart Study. *Circulation* 94: 2850–2855, 1996.
33. **Werle EO, Strobel G, Weicker H.** Decrease in rat cardiac β1- and β2-adrenoceptors by training and endurance exercise. *Life Sci* 46: 9–17, 1990.
34. **Williams RS.** Physical conditioning and membrane receptors for cardioregulatory hormones. *Cardiovasc Res* 14: 177–182, 1980.
35. **Williams RS, Schaible TF, Bishop T, Morey M.** Effects of endurance training on cholinergic and adrenergic receptors of rat heart. *J Mol Cell Cardiol* 16: 395–403, 1984.
36. **Yamamoto K, Miyachi M, Saitoh T, Yoshioka A, Onodera S.** Effects of endurance training on resting and post-exercise cardiac autonomic control. *Med Sci Sports Exerc* 33: 1496–1502, 2001.

AUTHOR QUERY FORM

ELSEVIER	**Journal: AUTNEU** **Article Number: 1288**	**Please e-mail or fax your responses and any corrections to:** **E-mail: corrections.esil@elsevier.spitech.com** **Fax: +1 619 699 6721**

Dear Author,

Any queries or remarks that have arisen during the processing of your manuscript are listed below and highlighted by flags in the proof. Please check your proof carefully and mark all corrections at the appropriate place in the proof (e.g., by using on-screen annotation in the PDF file) or compile them in a separate list.

For correction or revision of any artwork, please consult http://www.elsevier.com/artworkinstructions.

Any queries or remarks that have arisen during the processing of your manuscript are listed below and highlighted by flags in the proof. Click on the 'Q' link to go to the location in the proof.

Location in article	Query / Remark: click on the Q link to go Please insert your reply or correction at the corresponding line in the proof
Q1	Citation "Chao et al., 1999" has not been found in the reference list. Please supply full details for this reference.
Q2	The citation "Nakamoto et al., 2007" has been changed to match the author name/date in the reference list. Please check here and in subsequent occurrences, and correct if necessary.

Thank you for your assistance.

Autonomic Neuroscience: Basic and Clinical xxx (2010) xxx–xxx

Contents lists available at ScienceDirect

Autonomic Neuroscience: Basic and Clinical

journal homepage: www.elsevier.com/locate/autneu

Involvement of the mechanoreceptors in the sensory mechanisms of manual and electrical acupuncture

Hiromi Yamamoto [a,*], Toru Kawada [b], Atsunori Kamiya [b], Shunichi Miyazaki [a], Masaru Sugimachi [b]

[a] Division of Cardiology, Department of Medicine, Faculty of Medicine, Kinki University, Osaka, Japan
[b] Department of Cardiovascular Dynamics, National Cerebral and Cardiovascular Center Research Institute, Osaka, Japan

ARTICLE INFO

Article history:
Received 21 April 2010
Received in revised form 27 September 2010
Accepted 4 November 2010
Available online xxxx

Keywords:
Acupuncture
Arterial blood pressure
Heart rate
Mechanoreceptor
Gadolinium
Aortic depressor nerve

ABSTRACT

The modalities of acupuncture can be broadly classified into manual acupuncture (MA) and electroacupuncture (EA). Although MA has been reported to cause winding of tissue around the needle and subsequent activation of the sensory mechanoreceptors and nociceptors, the sensory mechanisms of acupuncture stimulation are not fully understood. To test the hypothesis that the involvement of the mechanoreceptors in the sensory mechanism is different in MA and EA, we examined the effects of a stretch-activated channel blocker gadolinium on the hemodynamic responses to hind limb MA and EA in anesthetized rats ($n=9$). Gadolinium significantly attenuated the MA-induced bradycardic response (-22 ± 5 vs. -10 ± 3 bpm, $P<0.05$) and tended to attenuate the MA-induced depressor response (-30 ± 5 vs. -18 ± 4 mm Hg, $P=0.06$). On the other hand, gadolinium significantly attenuated both the EA-induced bradycardic (-22 ± 5 vs. -9 ± 4 bpm, $P<0.01$) and depressor responses (-32 ± 6 vs. -15 ± 5 mm Hg, $P<0.01$). These results indicate that the mechanoreceptors are involved in the sensory mechanisms for both MA and EA.

1. Introduction

Acupuncture has been used to modulate autonomic nervous activity and cardiovascular function (Kimura and Sato, 1997; Lin et al., 2001). The modalities of acupuncture can be broadly classified into two categories: manual acupuncture (MA) and electroacupuncture (EA). MA and EA induce similar changes in the functional magnetic resonance imaging signal in the human brain (Napadow et al., 2005). Neural mechanisms involved in acupuncture have been the focus of investigations. The effects of EA are considered to be related to stimulation of finely myelinated (group III) and unmyelinated (group IV) fibers, which activate opioid receptors in the rostral ventrolateral medulla to inhibit sympathetic outflow (Chao et al., 1999). Depletion of group IV fibers by neonatal capsaicin treatment reduces the influence of EA on the pressor responses to mechanical stimulation of visceral organs (Tjen-A-Looi et al., 2005). The extensive network of tangential cutaneous axons, coupled with their communications with the large numbers of Merkel cells, might be considered a new division of the autonomic nervous system: the cutaneous intrinsic visceral afferent nervous system (Silberstein, 2009).

Although cardiovascular responses induced by acupuncture-like stimulation are known to be reflexes mediated via somatic afferent nerves, visceral afferent nerves and autonomic efferent nerves (Sato et al., 1994, 2002; Tjen-A-Looi et al., 2005; Uchida et al., 2007; Yamamoto et al., 2008; Silberstein, 2009), the sensory mechanisms of MA and EA that initiate afferent nerve discharge are not fully understood. Langevin et al. (2001) proposed that MA causes winding of tissues around the needle and subsequent activation of sensory mechanoreceptors and nociceptors, and also suggested that changes in extracellular milieu induced by MA are important factors for neuromodulation. Burnstock (2009) proposed that mechanical deformation of the skin leads to the release of ATP from keratinocytes, fibroblasts and other cells; then the sensory nerves are activated through purinergic receptors. Although EA may induce MA-like stimuli via electrical twitching of surrounding tissues, EA may also directly depolarize sensory axons and nerve terminals adjacent to the needle and induce reflex responses. If the direct depolarization is the major sensory mechanism of EA, inhibition of mechanoreceptors would not zsignificantly attenuate the effects of EA. On the other hand, if the mechanical stimulation plays a dominant role in the sensory mechanism of EA, inhibition of mechanoreceptors would significantly attenuate the effects of EA.

Among mechanoreceptors, mechanosensitive ion channels detect mechanical stimuli and transduce these stimuli into electrical signals in sensory neurons. Gadolinium chloride is widely used experimentally as an inhibitor of stretch-activated ion channels and physiological responses of tissues to mechanical stimulation (Adding et al., 2001). To test the hypothesis that the contribution of mechanoreceptors in the sensory mechanism differs in MA and EA, we examined the effects of gadolinium on the hemodynamic responses to MA and EA in anesthetized rats.

* Corresponding author. 377-2 Ohno-higashi, Osaka-sayama, Osaka 589-8511, Japan. Tel.: +81 72 366 0221; fax: +81 72 368 2378.
E-mail address: hiromi@med.kindai.ac.jp (H. Yamamoto).

1566-0702/$ – see front matter © 2010 Published by Elsevier B.V.
doi:10.1016/j.autneu.2010.11.004

2. Methods

2.1. Surgical preparation

Animal care was provided in strict accordance with the Guiding Principles for the Care and Use of Animals in the Field of Physiological Sciences approved by the Physiological Society of Japan. All protocols were reviewed and approved by the Animal Subject Committee at the National Cerebral and Cardiovascular Center. Male Wister Kyoto rats weighing from 310 to 460 g were anesthetized by an intraperitoneal injection of pentobarbital sodium (50 mg/kg) and ventilated mechanically via a tracheal tube with oxygen-enriched room air. The depth of anesthesia was maintained by continuous intravenous infusion of pentobarbital sodium (20–25 mg kg^{-1} h^{-1}) through a double lumen catheter inserted into the right external carotid vein. Ringer solution (6 mg kg^{-1} h^{-1}) was administered to maintain fluid balance. Arterial blood pressure (AP) was measured using a catheter inserted into the right common carotid artery. Heart rate (HR) was determined from AP using a cardiotachometer. Body temperature was maintained at approximately 38 °C using a heating pad.

2.2. MA and EA stimulations (n = 9)

With the animal in the supine position, both hind limbs were lifted to obtain a better view of the lateral sides of the lower legs. An acupuncture needle with a diameter of 0.2 mm (CE0123, Seirin-Kasei, Japan) was inserted into a point below the knee joint just lateral to the tibia in the left or right leg. For MA stimulation, the acupuncture needle was inserted to a depth of 5–10 mm and manually twisted clockwise and counter-clockwise, and moved up and down at a frequency of 1–2 Hz for a duration of 120 s. Two to three MA trials were conducted with an intervening interval of more than 5 min within which AP and HR returned to the respective pre-stimulation values. For EA stimulation, another acupuncture needle was inserted into a point approximately 1 cm from the above-mentioned needle toward the ankle joint and used as the ground. EA was applied for 120 s using an isolator connected to an electrical stimulator (SEN 7203, Nihon Kohden, Japan). The pulse width and the stimulus current were set at 500 μs and 5 mA, respectively. The stimulation frequency was set at 10 Hz in six and at 20 Hz in three of the nine rats. The pulse duration was based on previous studies (Tjen-A-Looi et al., 2005; Yamamoto et al., 2008; Uchida et al., 2008). The amplitude and frequency were selected so that the magnitudes of reflex hemodynamic responses became comparable to those induced by MA before gadolinium administration. In each animal, two to three EA trials were conducted with an intervening interval of more than 5 min within which AP and HR returned to the respective pre-stimulation values.

Gadolinium chloride hexahydrate was dissolved in saline at a concentration of 20 mM (Nakamoto and Matsukawa, 2007). After performing MA and EA under control conditions, we administered the gadolinium solution intravenously (2 ml/kg). After 10 min, we repeated MA and EA. The acupuncture needle positions were kept unchanged between MA and EA trials as well as before and after the gadolinium administration.

In a supplemental protocol (n = 7 additional rats), to examine the possibility that simple insertion of needles caused significant hemodynamic influences, an acupuncture needle (CE0123, Seirin-Kasei, Japan) was only inserted into a point below the knee joint just lateral to the tibia in the left or right leg and placed for a duration of 120 s. Needle was inserted to a depth of 5–10 mm.

2.3. Aortic depressor nerve stimulation (n = 6)

Using a pair of platinum electrodes, we identified the aortic depressor nerve (ADN) running along the common carotid artery, based on the AP pulse-synchronous nerve activity monitored through a loud speaker. After a depressor response to brief electrical stimulation of the nerve was confirmed, the electrodes and the nerve were fixed and insulated by silicone glue (Kwik-Sil, World Precision Instruments, FL, USA). The nerve fibers caudal to the electrodes were then crushed by a tight ligature so that only the afferent fibers directed to the central nervous system were stimulated. In four of the six rats, the right ADN was stimulated. In the remaining two rats, the left ADN was stimulated because of failure to stimulate the right ADN properly. The ADN was stimulated for 120 s at a frequency of 50 Hz (pulse width: 2 ms, voltage: 2 V). ADN stimulation was repeated with an interval of 5 min until the AP and HR responses appeared to be reproducible under control conditions. We then administered the gadolinium solution intravenously (20 mM, 2 ml/kg). After 10 min, we repeated the ADN stimulation.

2.4. Data analysis

Data were digitized using a 16-bit analog-to-digital converter (Contec, Japan) and stored at 200 Hz on a laboratory computer system. First, AP and HR data were averaged every 10 s. Averaged time courses of AP and HR responses were then obtained from two to three trials of MA, EA or ADN stimulation in each animal. Next, the effects of MA, EA or ADN were examined using repeated-measures one-way analysis of variance (ANOVA) followed by Dunnett's test (Glantz, 2002). The baseline data point immediately before stimulation was treated as a single control point for the Dunnett's test. Finally, the maximum effect of MA, EA or ADN stimulation was quantified by the differences between the minimum and baseline values for AP and HR (ΔAP and ΔHR). The effects of gadolinium on ΔAP and ΔHR were examined by a paired-t test (Glantz, 2002). The differences were considered significant at $P<0.05$. Data are presented in mean ± SE values.

3. Results

Fig. 1 depicts the averaged time courses of AP and HR responses to MA (n = 9 rats). MA gradually decreased AP and HR under control conditions. The minimum AP and HR were reached near the end of the MA stimulation period. After the cessation of MA, AP and HR gradually returned toward the respective baseline values. Intravenous gadolinium administration significantly decreased baseline AP from 138 ± 5 to 120 ± 5 mm Hg ($P<0.01$) but had no significant effect on baseline HR (379 ± 10 vs. 383 ± 7 bpm). Following gadolinium administration, although MA also decreased AP and HR significantly, ΔAP tended to be attenuated (−30 ± 5 vs. −18 ± 4 mm Hg; 68 ± 16% of the pre-gadolinium; $P=0.06$) and ΔHR was significantly attenuated (−22 ± 5 vs. −10 ± 3 bpm; 57 ± 23% of the pre-gadolinium; $P<0.05$) compared to control conditions.

Fig. 2 depicts the averaged time courses of AP and HR responses to EA (n = 9 rats). Under control conditions, EA decreased AP and HR. Both responses reached almost a steady state at approximately 1 min of EA stimulation. AP and HR remained decreased during the rest of the EA stimulation period, and gradually returned toward the respective baseline values after the cessation of EA. Intravenous gadolinium administration significantly decreased baseline AP from 140 ± 5 to 123 ± 7 mm Hg ($P<0.01$) but did not affect baseline HR (385 ± 9 vs. 384 ± 7 bpm). Following gadolinium administration, although EA significantly decreased AP, the decrease in HR was only significant at 55 s of EA stimulation. ΔAP (−32 ± 6 vs. −15 ± 5 mm Hg; 38 ± 11% of the pre-gadolinium; $P<0.01$) and ΔHR (−22 ± 5 vs. −9 ± 4 bpm; 37 ± 14% of the pre-gadolinium; $P<0.01$) were attenuated significantly compared to control conditions.

In the supplemental protocol (n = 7 rats), the insertion of an acupuncture needle alone did not significantly change AP (138 ± 9 vs. 138 ± 9 mm Hg) or HR (399 ± 20 vs. 400 ± 20 bpm).

Fig. 3 shows the averaged time courses of AP and HR responses to ADN stimulation (n = 6 rats). ADN stimulation decreased AP and HR under control conditions. The minimum AP and HR were reached at 15 s of ADN stimulation. Both parameters remained decreased during the rest of the ADN stimulation period, and returned toward the respective

Please cite this article as: Yamamoto, H., et al., Involvement of the mechanoreceptors in the sensory mechanisms of manual and electrical acupuncture, Auton. Neurosci. (2010), doi:10.1016/j.autneu.2010.11.004

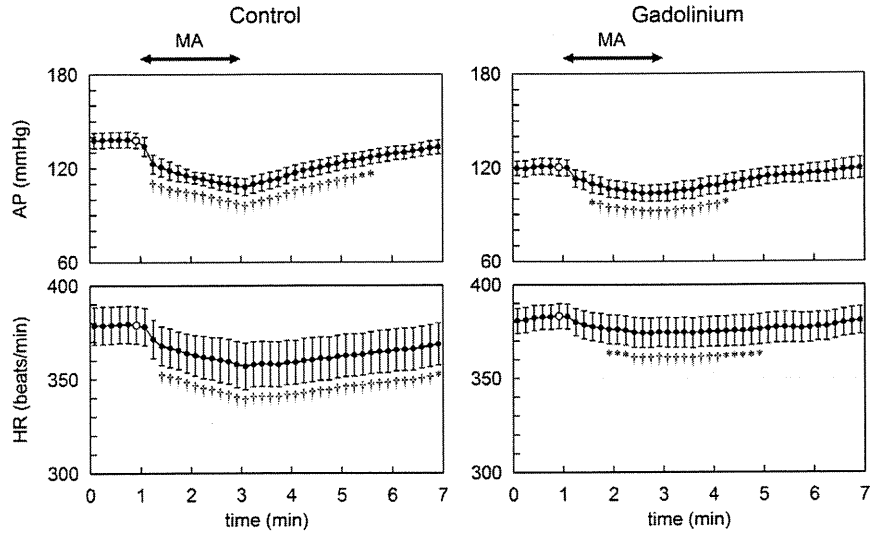

Fig. 1. Time courses of arterial pressure (AP) and heart rate (HR) responses induced by manual acupuncture (MA) averaged from 9 rats. MA gradually decreased AP and HR under control conditions (left) and after gadolinium administration (right). Gadolinium treatment tended to attenuate the AP response and significantly attenuated the HR response induced by MA, compared to control conditions. Data are mean ± SE values. *P<0.05 and †P<0.01 versus the control data point (open circle) immediately before the application of MA.

baseline values after the cessation of ADN stimulation. AP and HR appeared to recover more rapidly compared to those observed after MA and EA. Intravenous gadolinium administration significantly decreased baseline AP from 126 ± 4 to 118 ± 2 mm Hg (P<0.01) but had no significant effect on baseline HR (373 ± 13 vs. 369 ± 11 bpm). Following gadolinium administration, ADN stimulation significantly decreased AP and HR. Neither ΔAP (−43 ± 7 vs. −49 ± 3 mm Hg) nor ΔHR (−27 ± 8 vs. −34 ± 5 bpm) was attenuated compared to control conditions.

4. Discussion

We have shown that ion channels blocked by gadolinium are implicated in the hypotensive and bradycardic effects of acupuncture at the hind limb in rats, irrespective of technique.

4.1. Effects of gadolinium on AP and HR responses to MA and EA

Insertion of acupuncture needle alone did not change AP and HR significantly, indicating that continuous stimulation either by MA or EA was necessary to induce sustained AP and HR responses. Mechanoreceptors are thought to play an important role in the sensory mechanism of MA. Because gadolinium blocks mechanosensitive ion channels in sensory neurons (Cho et al., 2002), we hypothesized that intravenous administration of gadolinium would attenuate the AP and HR responses to MA. As expected, ΔAP tended to be attenuated after gadolinium administration (Fig. 1, top). However, since gadolinium also decreased baseline AP, it is uncertain whether the attenuation of ΔAP was mainly attributable to the inhibition of reflex response to MA or to the decreased baseline AP. On the other hand, gadolinium did not significantly affect baseline HR and

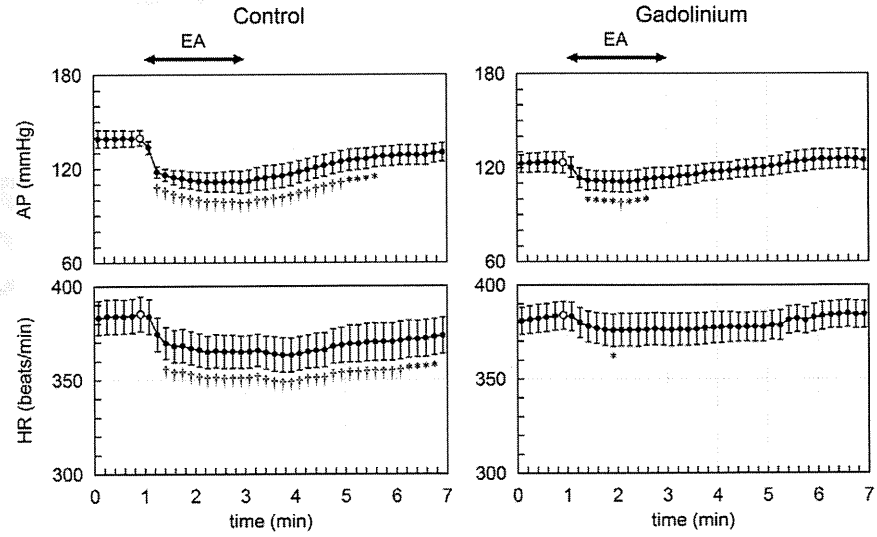

Fig. 2. Time courses of AP and HR responses induced by electroacupuncture (EA) averaged from 9 rats. EA gradually decreased AP and HR under control conditions (left) and after gadolinium administration (right). Gadolinium significantly attenuated both AP and HR responses induced by EA, compared to control conditions. Data are mean ± SE values. *P<0.05 and †P<0.01 versus the control data point (open circle) immediately before the application of EA.

Please cite this article as: Yamamoto, H., et al., Involvement of the mechanoreceptors in the sensory mechanisms of manual and electrical acupuncture, Auton. Neurosci. (2010), doi:10.1016/j.autneu.2010.11.004

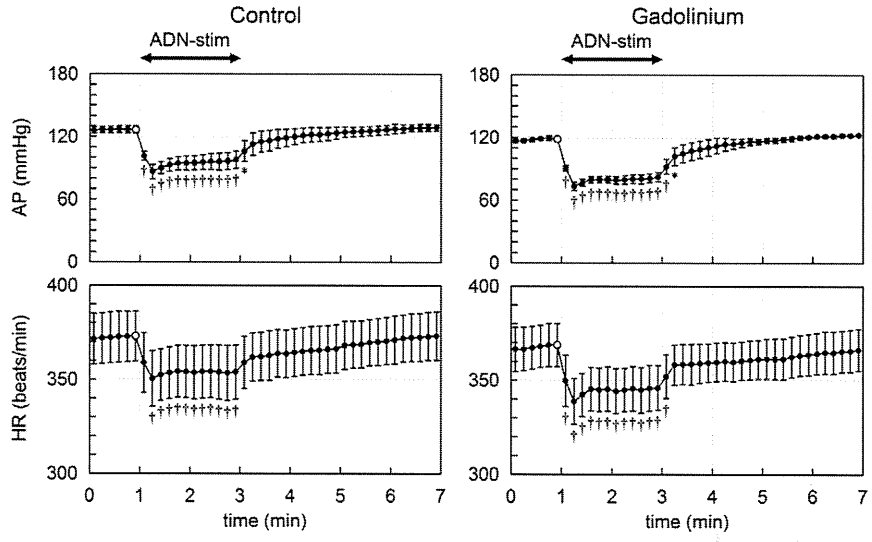

Fig. 3. Time courses of AP and HR responses induced by electrical stimulation of the aortic depressor nerve (ADN-stim) averaged from 6 rats. ADN-stim decreased AP and HR under control conditions (left) and after gadolinium administration (right). Gadolinium did not attenuate the AP and HR responses induced by ADN-stim, compared to control conditions. Data are mean ± SE values. *P<0.05 and †P<0.01 versus the control data point (open circle) immediately before the application of ADN-stim.

significantly attenuated ΔHR induced by MA (Fig. 1, bottom). Judging from the HR response, it is conceivable that gadolinium inhibits the reflex hemodynamic responses to MA.

We assumed that direct depolarization of sensory axons and nerve terminals adjacent to the needle could be the major sensory mechanism of EA. In fact, direct electrical stimulation of muscle afferent fibers evokes a variety of cardiovascular responses similar to those induced by EA (Sato et al., 1981). If direct depolarization is the major sensory mechanism for EA, inhibition of mechanoreceptors would have no significant effect on EA, because the results of the ADN stimulation protocol indicates that the axonal conduction would not be blocked even after gadolinium administration once the afferent nerve is discharged (Fig. 3). Contrary to this assumption, gadolinium significantly attenuated ΔAP and ΔHR induced by EA (Fig. 2), suggesting that the mechanoreceptors play an important role in the sensory mechanism of EA, as in the case of MA. EA probably causes electrical twitching of surrounding tissues and exerts MA-like stimulation through the mechanoreceptors.

Despite the significant contribution of mechanoreceptors to the sensory mechanisms of both MA and EA, the fact that the hemodynamic responses to MA and EA were not entirely abrogated after gadolinium administration indicates the presence of sensory mechanisms other than the mechanosensitive ion channels. Not all capsaicin-sensitive neurons are mechanosensitive, and gadolinium has no effect on capsaicin-induced calcium transient in sensory neurons (Gschossmann et al., 2000). Depletion of group IV fibers by neonatal capsaicin treatment reduces the influence of EA on the pressor responses to mechanical stimulation of visceral organs (Tjen-A-Looi et al., 2005), suggesting an importance of capsaicin-sensitive neurons in the mechanisms of acupuncture. Nociceptive neurons are therefore a likely candidate for the residual sensory mechanism after gadolinium administration. The group IV C-fiber tactile afferents is known to be widely distributed in the skin of mammals (Wessberg et al., 2003). These fibers could be regarded as a cutaneous intrinsic visceral afferent nervous system (Silberstein, 2009). In addition, the present results do not rule out the possibility that direct depolarization of sensory axons or nerve terminals occurs during EA. Albeit this assumption, EA seemed to have received even greater influence from gadolinium than MA (Figs. 1 and 2). Because MA with needle movements can cause greater deformations in the adjacent extracellular milieu compared to EA, MA may have induced signal transductions other than mechanosensitive ion channels, such as integrin-linked signal transduction pathways (Aplin et al., 1998), resulting in the greater residual hemodynamic responses after gadolinium administration. Further studies are required in the future to solve this question.

4.2. Effects of gadolinium on the AP and HR responses to ADN stimulation

Gadolinium decreased baseline AP, suggesting actions other than the inhibition of mechanosensitive ion channels. For instance, gadolinium has been shown to block voltage-gated calcium, sodium and potassium channels (Adding et al., 2001). To exclude the possibility that gadolinium attenuates the reflex hemodynamic responses to MA and EA via nonspecific mechanisms such as the inhibition of central autonomic neurotransmission, we performed the ADN stimulation experiment. Gadolinium did not attenuate ΔAP and ΔHR induced by ADN stimulation (Fig. 3). It is unlikely, therefore, that gadolinium inhibits the central autonomic neurotransmission from afferent to efferent nerve activities or significantly blunted the AP and HR responses to changes in autonomic nerve activities.

4.3. Implication of MA and EA

Although the present results indicate that MA and EA may share a common sensory mechanism, EA may be more flexible than MA in terms of its application for biomedical engineering because the effects of EA can be controlled quantitatively by adjusting the stimulation current and stimulation frequency. As an example, a previous study from our laboratories has demonstrated that servo-controlled hind limb electrical stimulation can reduce AP at a prescribed target level in anesthetized cats (Kawada et al., 2009). EA can be applied continuously using a stimulating device without the attendance of an acupuncturist once the needle is properly positioned. Continuous electrical stimulation of auricular acupuncture points for 48 h/week has been shown to be more effective than auricular acupuncture without electrical stimulation for the treatment of chronic cervical pain in an outpatient population (Sator-Katzenschlager et al., 2003). Although further studies are required, EA delivered via a dedicated stimulating device may be an additional modality to the treatment of cardiovascular diseases.

4.4. Limitations

First, the present study was conducted under pentobarbital anesthesia. Because anesthesia affects the autonomic tone, AP and HR

Please cite this article as: Yamamoto, H., et al., Involvement of the mechanoreceptors in the sensory mechanisms of manual and electrical acupuncture, Auton. Neurosci. (2010), doi:10.1016/j.autneu.2010.11.004

responses may differ when different anesthetics are used or when the animals are in a conscious state. However, as we compared the effects of gadolinium on the reflex responses to MA and EA under the same anesthetic conditions, the interpretation of the sensory mechanisms for MA and EA should be valid. Second, we performed EA at frequencies of 10 or 20 Hz in order to obtain AP and HR responses comparable to those observed during MA under control conditions. Because the effects of EA may differ depending on the magnitude of stimulation including pulse duration, current and frequency (Uchida et al., 2008; Kawada et al., 2009), further studies are needed to examine whether the effects of gadolinium on EA-induced hemodynamic responses vary depending on the stimulation intensities.

4.5. Conclusion

Intravenous administration of gadolinium attenuated the AP and HR responses to both MA and EA, suggesting that the mechanosensitive ion channels are involved in the sensory mechanisms of both MA and EA. EA may cause electrical twitching of surrounding tissues and induce MA-like stimulation through mechanoreceptors.

Acknowledgments

This study was supported by Health and Labour Sciences Research Grants (H19-nano-Ippan-009, H20-katsudo-Shitei-007, and H21-nano-Ippan-005) from the Ministry of Health, Labour and Welfare of Japan; by a Grant-in-Aid for Scientific Research (No. 20390462) from the Ministry of Education, Culture, Sports, Science and Technology of Japan; and by the Industrial Technology Research Grant Program from the New Energy and Industrial Technology Development Organization (NEDO) of Japan.

Appendix A

In an attempt to demonstrate that gadolinium does not significantly affect the hemodynamic responses to direct nerve stimulation related to acupuncture at the hind limb, we performed an additional protocol of tibial nerve stimulation in 5 anesthetized rats. The right tibial nerve was exposed and placed on a pair of platinum electrodes, and was stimulated for 120 s (500 μs, 10 Hz, 2 or 5 mA). ΔAP was -10.5 ± 3.5 mm Hg under baseline conditions, which was attenuated to -8.2 ± 4.4 mm Hg after gadolinium administration ($74 \pm 15\%$ of the pre-gadolinium, $P<0.01$). Although the relative reduction seemed smaller than that observed in EA ($38 \pm 11\%$ of the pre-gadolinium, see main text), because the reduction of ΔAP could be partly attributable to the decreased baseline AP after gadolinium administration, we could not judge whether gadolinium had truly inhibited the hypotensive effect of tibial nerve stimulation. Unfortunately, the tibial nerve stimulation did not change HR significantly in our experimental conditions ($\Delta HR = -1.1 \pm 4.4$ bpm before gadolinium vs. $\Delta HR = -1.4 \pm 4.1$ bpm after gadolinium), as opposed to a previous study (Uchida et al., 2008). As a result, we could not judge the effect of gadolinium based on HR either. We think the ADN stimulation protocol in the main text would be a second best surrogate to indicate the inability of gadolinium to block hemodynamic responses induced by direct activation of the afferent nerve.

References

Adding, L.C., Bannenberg, G.L., Gustafsson, L.E., 2001. Basic experimental studies and clinical aspects of gadolinium salts and chelates. Cardiovasc. Drug Rev. 19, 41–56.

Aplin, A.E., Howe, A., Alahari, S.K., Juliano, R.L., 1998. Signal transduction and signal modulation by cell adhesion receptors: the role of integrins, cadherins, immunoglobulin-cell adhesion molecules, and selectins. Pharmacol. Rev. 50 (2), 197–263.

Burnstock, G., 2009. Acupuncture: a novel hypothesis for the involvement of purinergic signalling. Med. Hypotheses 73, 470–472.

Cho, H., Shin, J., Shin, C.Y., Lee, S., Oh, U., 2002. Mechanosensitive ion channels in cultured sensory neurons of neonatal rats. J. Neurosci. 22 (4), 1238–1247.

Glantz, S.A., 2002. Primer of Biostatistics, 5th ed. McGraw-Hill, New York.

Gschossmann, J.M., Chaban, V.V., McRoberts, J.A., Raybould, H.E., Young, S.H., Ennes, H.S., Lembo, T., Mayer, E.A., 2000. Mechanical action of dorsal root ganglion cells in vitro: comparison with capsaicin and modulation by kappa-opioids. Brain Res. 856 (1–2), 101–110.

Kawada, T., Shimizu, S., Yamamoto, T., Shishido, T., Kamiya, A., Miyamoto, T., Sunagawa, K., Sugimachi, M., 2009. Servo-controlled hind-limb electrical stimulation for short-term arterial pressure control. Circ. J. 73 (5), 851–859.

Kimura, A., Sato, A., 1997. Somatic regulation of autonomic functions in anesthetized animals—neural mechanisms of physical therapy including acupuncture. Jpn J. Vet. Res. 45 (3), 137–145.

Langevin, H.M., Churchill, D.L., Cipolla, M.J., 2001. Mechanical signaling through connective tissue: a mechanism for the therapeutic effect of acupuncture. FASEB J. 15, 2275–2285.

Lin, M.C., Nahin, R., Gershwin, M.E., Longhurst, J.C., Wu, K.K., 2001. State of complementary and alternative medicine in cardiovascular, lung, and blood research: executive summary of a workshop. Circulation 103 (16), 2038–2041.

Nakamoto, T., Matsukawa, K., 2007. Muscle mechanosensitive receptors close to the myotendinous junction of the Achilles tendon elicit a pressor reflex. J. Appl. Physiol. 102, 2112–2120.

Napadow, V., Makris, N., Liu, J., Kettner, N.W., Kenneth, K.K., Hui, K.K.S., 2005. Effects of electroacupuncture versus manual acupuncture on the human brain as measured by fMRI. Hum. Brain Mapp. 24, 193–205.

Sato, A., Sato, Y., Schmidt, R.F., 1981. Heart rate changes reflecting modifications of efferent cardiac sympathetic outflow by cutaneous and muscle afferent volleys. J. Auton. Nerv. Syst. 4 (3), 231–247.

Sato, A., Sato, Y., Suzuki, A., Uchida, S., 1994. Reflex modulation of gastric and vesical function by acupuncture-like stimulation in anesthetized rats. Biomed. Res. 15, 59–65.

Sato, A., Sato, Y., Uchida, S., 2002. Reflex modulation of visceral functions by acupuncture-like stimulation in anesthetized rats. Int. Congr. Ser. 1238, 111–123.

Sator-Katzenschlager, S.M., Szeles, J.C., Scharbert, G., Michalek-Sauberer, A., Kober, A., Heinze, G., Kozek-Langenecker, S.A., 2003. Electrical stimulation of auricular acupuncture points is more effective than conventional manual auricular acupuncture in chronic cervical pain: a pilot study. Anesth. Analg. 97, 1469–1473.

Silberstein, M., 2009. The cutaneous intrinsic visceral afferent nervous system: a new model for acupuncture analgesia. J. Theor. Biol. 261, 637–642.

Tjen-A-Looi, S.C., Fu, L.-W., Zhou, W., Syuu, Z., Longhurst, J.C., 2005. Role of unmyelinated fibers in electroacupuncture cardiovascular responses. Auton. Neurosci. 118, 43–50.

Uchida, S., Shimura, M., Ohsawa, H., Suzuki, A., 2007. Neural mechanism of bradycardic responses elicited by acupuncture-like stimulation to a hind limb in anesthetized rats. J. Physiol. Sci. 57 (6), 377–382.

Uchida, S., Kagitani, F., Hotta, H., 2008. Mechanism of the reflex inhibition of heart rate elicited by acupuncture-like stimulation in anesthetized rats. Auton. Neurosci. 143, 12–19.

Wessberg, J., Olausson, H., Fernstrom, W.F., Vallbo, B.A., 2003. Receptive field properties of unmyelinated tactile afferents in the human skin. J. Neurophysiol. 89, 1567–1575.

Yamamoto, H., Kawada, T., Kamiya, A., Kita, T., Sugimachi, M., 2008. Electroacupuncture changes the relationship between cardiac and renal sympathetic nerve activities in anesthetized cats. Auton. Neurosci. 144 (1–2), 43–49.

Please cite this article as: Yamamoto, H., et al., Involvement of the mechanoreceptors in the sensory mechanisms of manual and electrical acupuncture, Auton. Neurosci. (2010), doi:10.1016/j.autneu.2010.11.004

33rd Annual International Conference of the IEEE EMBS
Boston, Massachusetts USA, August 30 - September 3, 2011

Reduction of Myocardial Oxygen Demand by Controlling Heart Rate and Hemodynamics Simultaneously by Novel Circulatory Model

Masaru Sugimachi, *Member, IEEE*, Kazunori Uemura, Toru Kawada, Toshiaki Shishido, and Kenji Sunagawa, *Member, IEEE*

***Abstract*—We were already capable of restoring automatically blood pressure, cardiac output, and left atrial pressure by an inotropic, a vasodilator, and volume infusion/a diuretic. Countermeasures for cardioprotection, however, should be integrated to improve the long-term outcomes. We established a full control of heart rate and examined if such a control was useful for decreasing cardiac oxygen consumption. Based on a simulation result, we conducted an animal experiment. In 7 dogs with acute heart failure, we treated hemodynamics, and then lowered heart rate. Compared to the treatment for hemodynamics alone, the addition of bradycardia decreased cardiac oxygen consumption. It was possible to maintain hemodynamics without sacrificing cardiac oxygen consumption.**

I. Introduction

THE ultimate goal of the treatment of acute failure is the restoration of failing hemodynamics. Although the native regulation for the cardiovascular system plays a role to sustain normal blood pressure when the severity of heart failure is mild (called compensated heart failure), the ability of native regulation is limited. To sustain life, not only blood pressure, but also peripheral perfusion (indexed by cardiac output) and the absence of pulmonary edema (indexed by low left atrial pressure) are necessary. The native regulation fails to restore cardiac output and left atrial pressure in advanced heart failure.

We have shown that with the use of an inotropic agent, a vasodilator, and volume infusion/a diuretic, we were able to restore automatically all of blood pressure, cardiac output, left atrial pressure [1]. In this study, the peripheral demand was fulfilled. The overload on the heart was, however, not ameliorated. Countermeasures for cardioprotection should probably also be a part of the treatment and should be integrated, so as to improve the long-term outcomes of the patient recovering from acute heart failure.

Manuscript received April 13, 2011. This work was supported in part by Grant-in-Aid for Scientific Research (B 20300164) from the Ministry of Education, Culture, Sports, Science and Technology, by Health and Labour Sciences Research Grants (H20-katsudo-shitei-007) from the Ministry of Health Labour and Welfare of Japan (corresponding author Masaru Sugimachi, MD, PhD to provide phone: +81-6-6833-5012; fax: +81-6-6835-5403; e-mail: su91mach@ri.ncvc.go.jp).

M. Sugimachi, K. Uemura, T. Kawada, and T. Shishido are with the National Cerebral and Cardiovascular Center Research Institute, Suita, Osaka 5658565, Japan.

K. Sunagawa is with Kyushu University, Fukuoka 8128582 Japan.

We have already used the control of left ventricular contractility, systemic vascular resistance and blood volume to automatically restore blood pressure, cardiac output, and left atrial pressure. For the cardioprotection, we have to use the control of another cardiovascular property. We focused on the control of heart rate and examined if this was useful for the cardioprotection. We assumed here that low minute left ventricular oxygen consumption can be used as an index for cardioprotection.

II. Theoretical Analysis

A. Definition of the Problem

To supply the peripheral demand and to prevent pulmonary congestion, the cardiovascular system needs to operate with sufficiently high mean blood pressure (P_m), large cardiac output (CO), and low left atrial pressure (P_{LA}). Considering the physiologically normal values, we fixed P_m to 100 mmHg, CO to 100 $ml \cdot min^{-1} \cdot kg^{-1}$, and P_{LA} to 10 mmHg.

Even with these multiple constraints, the cardiovascular system does not operate with a unique condition. It can operate with various sets of contractility and heart rate (*see the next subsection B*). We simulated these various hemodynamics, and searched for the condition to minimize minute LV oxygen consumption [2].

B. Hemodynamics

We used left ventricular (LV) end-systolic pressure-volume relationship (ESPVR) and the framework of ventricular-arterial coupling to reproduce hemodynamics [3]. We approximated LV ESPVR by a straight line, and coupled end-systolic elastance (E_{es}) with effective arterial elastance (E_a). E_a was approximated by R/T, where R was systemic vascular resistance and T was heart period, reciprocal of heart rate (HR).

Using these approximations, for a given LV end-diastolic stressed volume (V_{eds}), stroke volume (SV) and CO can be calculated as

$$SV = V_{eds} \frac{T \cdot E_{es}}{T \cdot E_{es} + R} \quad (1)$$

$$CO = V_{eds} \frac{E_{es}}{T \cdot E_{es} + R} \quad (2).$$

LV end-systolic stressed volume (V_{ess}) and pressure (P_{es})

can be calculated as

$$V_{ess} = V_{eds} \frac{R}{T \cdot E_{es} + R} \quad (3)$$

$$P_{es} = V_{eds} \frac{E_{es} \cdot R}{T \cdot E_{es} + R} \quad (4).$$

In the framework of ventricular-arterial coupling, P_m was approximated by P_{es}. Systemic vascular resistance, R was therefore given by 1 mmHg·ml^{-1}·min·kg. Also, as P_{LA} was approximated by LV end-diastolic pressure (P_{ed}), V_{eds} would be calculated if we assume a predefined LV end-diastolic pressure-volume relationship (EDPVR). In this analysis, we used an exponential LV EDPVS as follows (V_{eds} in mL, P_{ed} in mmHg)

$$P_{ed} = \exp(0.082 \cdot V_{eds} - 0.8) + 2.03 \quad (5),$$

corresponding to the EDPVR with P_{ed} of 10 mmHg for V_{eds} of 35 ml.

Knowing R and V_{eds}, a necessary relationship between LV contractility (E_{es}) and heart period (T, an inverse of heart rate) is obtained. Even though it is necessary to follow this relationship to maintain P_m, CO, and P_{LA}, not a unique set of E_{es} and T would be obtained. Rather multiple sets of E_{es} and T would be feasible (*see the previous subsection A*).

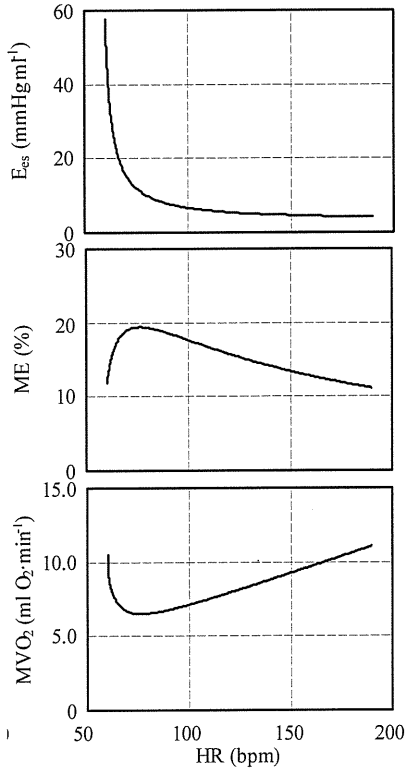

Fig. 1. Simulated relations of heart rate (HR) with left ventricular end-systolic elastance (E_{es}) (top), left ventricular mechanical efficiency (ME) (middle), and minute left ventricular oxygen consumption (MVO_2) (bottom), when mean blood pressure, cardiac output and left atrial pressure are kept at fixed values

C. Myocardial Oxygen Consumption

Beat LV oxygen consumption (BVO_2) was determined by PVA and E_{es} with high precision as follows [4]

$$BVO_2 = \alpha \cdot PVA + \beta \cdot E_{es} + \gamma \quad (6)$$

where α (1.8×10^{-5} mL O_2·mmHg^{-1}·mL^{-1}), β (1.8×10^{-3} mL O_2·mmHg^{-1}·mL), and γ (1.0×10^{-2} mL O_2) are constants. PVA stands for LV pressure-volume area (an index of total mechanical energy of LV contraction). PVA is the sum of LV stroke work (SW) and potential energy (PE). SW and PE are approximated as

$$SW = (P_m - P_{LA}) \cdot CO / HR \quad (7)$$

$$PE = P_{LA}^{\ 2} / 2E_{es} \quad (8).$$

Minute LV oxygen consumption per minute (MVO_2) and LV mechanical efficiency (ME) and are expressed as follows

$$MVO_2 = BVO_2 \cdot HR \quad (9)$$

$$ME = SW / BVO_2 = SW \cdot HR / MVO_2 \quad (10).$$

D. Simulation Results

Shown in Fig. 1 are simulation results. As explained in *subsection B*, there is an inverse relationship between E_{es} and heart rate [HR]. The top panel shows that if the heart is made bradycardiac, LV contractility should be enhanced to maintain P_m, CO, and P_{LA}, or to meet the peripheral demands.

The middle and the bottom panel show that ME would increase and MVO_2 would decrease by making heart bradycardiac up to a certain HR. Below this HR, however, rather ME would decrease and MVO_2 would increase with further decrease in HR. The differences in constants α, β and γ would change the optimal HR but would not change the basic relations show in Fig. 1.

E. Interpretation of the Simulation Results

As predicted by Eqs. 6 and 9, MVO_2 would largely be affected by HR. As MVO_2 is obtained by multiplying BVO_2 by HR, and as BVO_2 does not decrease much with HR, MVO_2 increases with HR.

In extreme bradycardiac condition, however, increase in E_{es} is so rapid, and the effect of increase in E_{es} overwhelmed the effect of HR.

ME is shown to be proportional to the reciprocal of MVO_2. Using, Eq. 7, the numerator of the right-hand side of Eq. 10, SW·HR is equal to (P_m-P_{LA})·CO and is constant.

III. Animal Experiment

We reproduced a similar condition as the previous simulation and examined if the same results would be obtained in an animal experiment [5].

A. Methods

We used 7 dogs for this animal experiment. These dogs were anesthetized and underwent coronary micro-embolization with glass beads. This procedure resulted in acute ischemic heart failure. We adjusted the size and the

dose of the emboli, so as to create heart failure severe enough that necessitated an intensive care. In these dogs, CO decreased by 39% (from 101±5 to 62±13 ml·min^{-1}·kg^{-1}), P_m decreased by 17 mmHg (from 114±4 to 97±14 mmHg), and P_{LA} increased by 8 mmHg (from 9 ± 1 to 17±2 mmHg).

To take the full control of HR in hand, a specific bradycardiac agent zatebradine (0.5 mg·kg^{-1}) was administered intravenously, and the intrinsic atrial beats were suppressed. Then, HR is fully controlled by atrial pacing. We first set HR at the rate before zatebradine infusion (146±8 bpm). In this condition (designated as *untreated*), we measured hemodynamics and cardiac energetics.

We then activated the autopilot system [1] we developed to maintain the desired P_m, CO, and P_{LA}. We customized in each animal the target values for P_m, CO, and P_{LA}. These ranged between 90 to 100 mmHg for P_m, 80 to 100 ml·min^{-1}·kg^{-1} for CO, and 10 to 12 mmHg for P_{LA}. The system restored P_m, CO and P_{LA} to their respective target values within 30 min. After confirming stable hemodynamics, (designated as *treated for hemodynamics*), we measured hemodynamics and cardiac energetics.

After the treatment of hemodynamics, we then reduced the atrial pacing rate in steps of 10 or 20 bpm. For each HR step, we waited until the hemodynamics stabilized. . We were able to reduce HR by 39±12 bpm. We measured hemodynamics and cardiac energetics at the lowest HR and stable hemodynamics (designated as *treated for hemodynamics and energetics*).

B. Results

We summarized the results of the animal experiment in Fig. 2. In each panel we plotted the pooled relationships between HR and various indexes of hemodynamics and cardiac energetics, in 7 dogs.

In *Untreated* condition (shown by open circles), CO was lower and P_{LA} was higher than normal. P_m was not so different from normal values. HR was quite high due to the activation of sympathetic nervous system.

By activating the autopilot system (*Treated for Hemodynamics* condition, shown by solid triangle), CO and P_{LA} were restored to the target normal values. P_m was slightly decreased. Because we are fully controlling HR, and we did not change the setting of HR, HR remained high also in this condition.

After decreasing HR to the lowest level (*Treated for Hemodynamics and Energetics* condition, shown by solid circle), all of CO, P_{LA}, and P_m remained the target normal values despite the large decrease in HR (CO: 89 ± 3 ml·min^{-1}·kg^{-1} to 88 ± 3 ml·min^{-1}·kg^{-1}, P_{LA}: 10.5 ± 0.4 mmHg to 10.9 ± 0.4 mmHg, P_m: 94 ± 3 mmHg to 93 ± 2 mmHg, all NS).

As shown in the right upper panel, the treatment for hemodynamics required the enhancement of contractility (E_{es}, $p<0.05$ vs. *Treated for Hemodynamics*); this is accomplished by the automatic infusion of a positive inotropic agent (dobutamine, increased from 1.4 ± 0.3 to 2.7 ± 0.5 μg·min^{-1}·kg^{-1}, $p<0.01$). With a decrease in heart rate, it is shown that a further increase in contractility was necessary to maintain CO, P_{LA}, and P_m. Doses for other drugs were also changed to maintain hemodynamics.

Although ME increased with the treatment for hemodynamics, this was at the expense of increasing MVO_2. With the treatment of hemodynamics and energetics, however, we were able to maintain hemodynamics, further improving ME ($p<0.01$ vs. *Treated for Hemodynamics*), and at the same time decreasing MVO_2 almost at the untreated level or rather to a lower level ($p<0.01$ vs. *Treated for Hemodynamics*). Even though we were unable to study extreme bradycardiac condition, a similar relationships were obtained as the theoretical analysis up to the heart rate studied (i.e., minimal heart rate was not below the optimal heart rate for minimizing myocardial oxygen consumption).

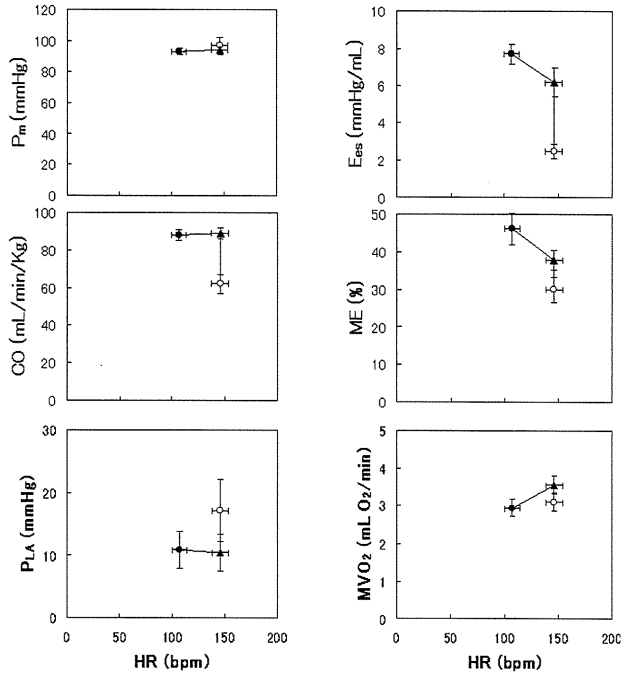

Fig. 2. Pooled relations between heart rate (HR) and mean blood pressure (P_m) (left top), cardiac output (CO) (left middle), left atrial pressure (P_{LA}) (left bottom), end-systolic elastance (E_{es}) (right top), left ventricular mechanical efficiency (ME) (right middle), and minute left ventricular oxygen consumption (MVO_2) (right bottom) in 7 dogs

IV. Conclusion

By taking full control of heart rate, and by adjusting treatment for hemodynamics at the same time, it was possible to maintain hemodynamics without sacrificing LV oxygen consumption.

REFERENCES

[1] K. Uemura, A. Kamiya, I. Hidaka, T. Kawada, S. Shimizu, *et al.*, "Automated drug delivery system to control systemic arterial pressure, cardiac output, and left heart filling pressure in acute decompensated heart failure," *J. Appl. Physiol.* vol. 100, no 4, 1278-1286, Apr. 2006.

[2] M. Sugimachi, K. Todaka, K. Sunagawa, M. Nakamura, "Optimal afterload for the heart vs. optimal heart for the afterload," *Front. Med. Biol. Eng.* vol. 2, no. 3, 217-221, 1990.

[3] K. Sunagawa, K. Sagawa, W. L. Maughan, "Ventricular interaction with the loading system," *Ann. Biomed. Eng.* vol. 12, no. 2, 163-189, 1984.

[4] H. Suga, "Ventricular energetics," *Physiol. Rev.* vol. 70, no. 2, 247-277, Apr. 1990.

[5] K. Uemura, K. Sunagawa, M. Sugimachi, "Computationally managed bradycardia improved cardiac energetics while restoring normal hemodynamics in heart failure," *Ann. Biomed. Eng.* vol. 37, no. 1, 82-93, Jan. 2009.

33rd Annual International Conference of the IEEE EMBS
Boston, Massachusetts USA, August 30 - September 3, 2011

Impact of baroreflex on venous return surface

Takafumi Sakamoto, Yoshinori Murayama, Atsushi Tanaka, Kazuo Sakamoto, Tomoyuki Tobushi, Keita Saku, Kazuya Hosokawa, Ken Onitsuka, Takeo Fujino and Kenji Sunagawa, Senior *Member, IEEE*

Abstract— **Background: Although Guyton's concept of venous return (VR) revolutionized circulatory physiology, the pulmonary circulation is invisible in its original framework. Since the pulmonary circulation is critical in left heart failure, we characterized the VR as a surface described by right (P_{RA}) and left atrial (P_{LA}) pressures and demonstrated that the VR surface was capable of representing mechanics of pulmonary as well as systemic circulation. However how baroreflex impacts the VR surface remains unknown. Methods/Results: In 8 dogs, we isolated the carotid sinuses and replaced both ventricles with pumps. We varied cardiac output, shifted blood distribution between the systemic and pulmonary circulation at carotid sinus pressures (CSP) of 100 or 140 mmHg. The coefficient of determination of the VR surface ranged 0.96-0.99 indicating how flat the surface is. Increasing CSP decreased maximum VR (233±27 vs. 216±33 ml/kg/min, $p<0.05$), whereas did not change the slopes of VR along P_{RA} or P_{LA} axes. Conclusions: Baroreflex parallel shifts the VR surface, thereby stressed volume, without changing its slopes.**

I. Introduction

Guyton's classic concept of circulatory equilibrium [1] revolutionized circulatory physiology. Guyton's classic concept, however, was not intended to represent the circulatory equilibrium of left ventricular failure because neither left ventricular mechanics nor pulmonary circulation is explicitly incorporated. To overcome such a limitation of Guyton's classic concept, we previously developed a framework of circulatory equilibrium [2, 3] where, as shown in Fig. 1, we defined the cardiac output curve and venous return curve as functions of both right atrial pressure (P_{RA}) and left atrial pressure (P_{LA}). We denoted the venous return curve as the venous return surface. A theoretical analysis using a distributed vascular model indicated that venous return (VR) of the total circulatory system can be described as

$$VR=VR_{max}-(G_P P_{LA}+G_S P_{RA}) \qquad (1)$$

where VR_{max} is maximum venous return and is a function of stressed blood volume [2, 3, 4], G_P and G_S, conductance of pulmonary and systemic venous return, respectively. We demonstrated that the venous return surface was remarkably flat and the slopes toward the P_{LA} and P_{RA} axes did not differ among animal preparations [2, 3].

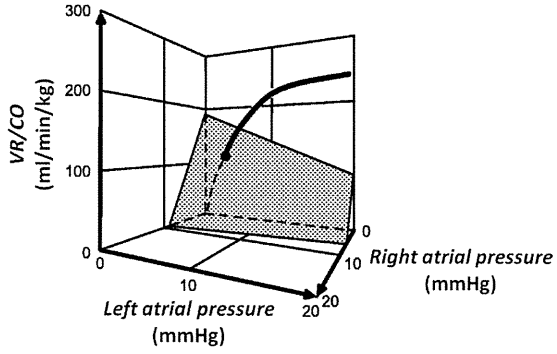

Figure 1 Proposed framework of circulatory equilibrium consists of integrated cardiac output curve and venous return surface.

Since baroreflex is a powerful physiological modulator of mechanical properties of cardiovascular system and thereby capable of changing circulatory equilibrium, we investigated how baroreflex impacts on characteristics of venous return surface.

II. Methods

A. Animal preparation

Eight mongrel dogs were anesthetized with pentobarbital sodium and ventilated artificially. We isolated the bilateral carotid sinuses from the systemic circulation and connected them to a servo-controlled piston pump to control intra-carotid sinus pressure (CSP). We cut the bilateral vagosympathetic trunks to eliminate other reflexes. After median sternotomy, the heart was suspended in a pericardial cradle. Fluid-filled catheters were placed in the right and left atrium to measure pressures.

To examine the venous return surface, we performed total heart bypass. Two roller pumps were used to control systemic and pulmonary flows. A systemic perfusion cannula was placed in the right common carotid artery. A draining cannula for the systemic circulation was inserted into the right ventricle through its free wall. A pulmonary perfusion cannula was placed in the pulmonary artery. A draining cannula for pulmonary circulation was inserted into the left ventricle via the apex. The flow rate (i.e., cardiac output) was measured by an in-line ultrasonic flow probe. After starting two roller pumps at a matched rate, we tied an umbilical tape around pulmonary artery, clamped the ascending aorta and thus established the total heart bypass.

B. Protocol

For a given CSP, we waited for several minutes until the

Manuscript received September 15, 2011. This work was supported in part by Health and Labour Sciences Research Grant for Research on Medical Devices for Improving Impaired QOL from the Ministry of Health Labour and Welfare of Japan, Health and Labour Sciences Research Grant for Clinical Research from the Ministry of Health Labour and Welfare of Japan, and Grant-in-Aid for Scientific Research(S) (18100006) from the Japan Society for the Promotion of Science

All authors are with Kyushu University, Fukuoka 8128582 Japan. (corresponding author Takafumi Sakamoto to provide phone: +81-92-642-5360; fax: +81-92-642-5357; e-mail: tsaka@cardiol.med.kyushu-u.ac.jp).